Contrast-Enhanced MR Angiography

Jeffrey H. Maki, MD, PhD; Michael V. Knopp, MD, PhD; Martin Prince, MD, PhD

Rapid advances in the implementation and understanding of three-dimensional (3D) contrast-enhanced magnetic resonance angiography (CE-MRA) are making minimally invasive vascular imaging safer and more accurate. For this reason, CE-MRA is increasingly utilized as the primary method of vascular imaging. This article describes the basic principles underlying 3D CE-MRA and demonstrates applications throughout the body. Inherent advantages of 3D contrast MRA over "conventional" MRA techniques, such as time-of-flight (TOF) and phase contrast (PC), will be discussed. Furthermore, we will explore techniques for improving spatial and temporal resolution, reducing respiratory motion artifacts, decreasing contrast dosing, and more accurately timing the contrast bolus. Finally, new contrast agents will be reviewed briefly.

CONVENTIONAL MRA

MR pulse sequences can exploit blood motion to visualize vascular structures directly without intravascular contrast material. One of the earliest MRA techniques, TOF angiography, is performed using a flow-compensated, gradient-refocused sequence. Data can be acquired as multiple two-dimensional (2D) slices, or as a single 3D volume. In this technique, stationary tissues in the slice or volume of interest are "saturated" and, therefore, have low signal intensity.[1-3] Blood upstream of the imaging volume, however, remains "unsaturated." When this blood flows into the imaging volume, it is bright compared with the stationary background tissues. This "in-flow" or TOF approach often works particularly well in relatively normal arteries and veins, including the inferior vena cava (IVC), iliac veins, carotid arteries, and cerebral vasculature.[4-12] It also has the benefit of allowing selective saturation of blood adjacent to the imaging volume such that either arterial or venous signal can be suppressed. One major disadvantage of TOF angiography is in-plane saturation, which can be a problem with slowly flowing blood in tortuous arteries or when the long axis of the vessel coincides with the scan plane. A second limitation is turbulence-induced signal loss in and distal to a stenosis.[13,14] In addition, the relatively long echo times required for gradient moment nulling make TOF sensitive to susceptibility artifacts from metallic clips, metal implants, and bowel gas or other air-tissue interfaces. These artifacts have been implicated as a primary reason for inaccuracy in TOF MRA. As a further

Dr. Maki is an Associate Professor in the Department of Radiology, University of Washington, Seattle, WA. Dr. Knopp is a Professor in the Department of Radiology, The Ohio State University Hospitals, Columbus, OH. Dr. Prince is a Professor in the Department of Radiology, Weill Medical College of Cornell University, and Columbia College of Physicians and Surgeons, New York, NY.

CME CATEGORY 1

This CME program is sponsored by an educational grant grom Bracco Diagnostics Inc.

The Institute for Advanced Medical Education designates this continuing medical education activity for a maximum of 3 Category 1 credits toward the AMA Physician's Recognition Award. Each physician should claim only those credits that he/she actually spent in the activity.

This CME article consists of text and related images appearing in this journal article and online at *www.appliedradiology.com.* You should read the articles and accompanying images, refer to the references, and complete the self-evaluation quiz available online at *www.appliedradiology.com.* There is no charge for participating in this program.

Estimated time for completion: Three hours

Date of release: April 2003

Expiration date: April 2005

Program: MH-003

LEARNING OBJECTIVES

After completing this activity, the reader will:

- Be familiar with general parameters/techniques for performing 3D CE-MRA in the carotid, aortic, pulmonary, pelvic, renal, mesenteric, and peripheral arteries, as well as the portal and peripheral veins
- Have a general understanding of k-space and artifacts, and understand the significance of sequential vs. centric acquisition order
- Understand the importance of proper bolus timing as related to 3D CE-MRA, and know the different ways to achieve that timing
- Be familiar with some of the new contrast agents currently under investigation, and understand how they may apply to future MRA applications

downside, TOF imaging times tend to be lengthy. This is due to the need to image perpendicular to the vessel axis in order to avoid in-plane saturation. Long acquisition times can lead to motion artifacts, including slice misregistration, particularly for those patients who have difficulty remaining still.

Phase-contrast (PC) angiography makes use of phase shifts as blood flows in the presence of flow-encoding gradients.[1,15,16] Using phase-difference images (created by subtracting two images created with opposite flow-encoding gradients), residual phase is proportional to velocity. Stationary background tissue, however, is suppressed because it has no phase shift on either image, and hence subtracts completely. The flow-encoding gradients can be applied in any direction, or in multiple directions, depending on the desired flow sensitivity. Phase-contrast angiography can be implemented as a 2D or 3D gradient-refocused sequence, and is substantially improved when performed after contrast administration.[17] It has proven useful for evaluation of the renal arteries, carotid arteries, and the portal vein.[8,12,16-20] In normal vessels without stenoses or turbulence, the results are often spectacular.

Another strength of PC angiography is its ability to measure flow velocities. In combination with cine (synchronization with cardiac gating), a time-resolved velocity profile can be generated similar to an ultrasound Doppler waveform.[21,22] This provides physiologic flow data and allows for the quantitative measurement of flow rates. Unfortunately, it is this same velocity sensitivity that limits PC angiography. Strong flow-encoding gradients make the sequence susceptible to degradation from bulk (cardiac, respiratory, translational) motion. In addition, PC sequences only quantify a specified range of velocities.[19] In occlusive disease, turbulence causes a broad spectrum of rapidly varying velocities, which in turn causes intravoxel phase dispersion and signal loss. Thus, artifactual loss of vessel visualization at a stenosis is common.[13] Interestingly, this apparent deficiency can be useful as an adjunct to 3D CE-MRA for characterizing the hemodynamic significance of a stenosis, as pressure gradients are known to occur in regions of high turbulence and jet-flow.

CONTRAST-ENHANCED MRA: THEORY

Three-dimensional CE-MRA is performed in a manner analogous to conventional contrast angiography or helical computed tomography (CT). Rather than relying on blood motion to create intravascular signal, a contrast agent (traditionally a gadolinium chelate) is introduced to shorten the T1 (spin lattice) relaxation time of blood such that it is significantly less than the surrounding tissues. Blood can then be imaged directly (using a T1-weighted sequence), irrespective of flow effects. This alleviates many of the problems inherent to TOF and PC angiography. In particular, sensitivity to turbulence is dramatically reduced, and in-plane saturation effects are eliminated.[13,14] The technique allows a small number of slices to be oriented in the plane of the target vessels to quickly image an extensive region of vascular anatomy (equal to the field-of-view) at high in-plane resolution. Thus, 3D CE-MRA is intrinsically fast, allowing high-quality breath-hold MR angiograms.

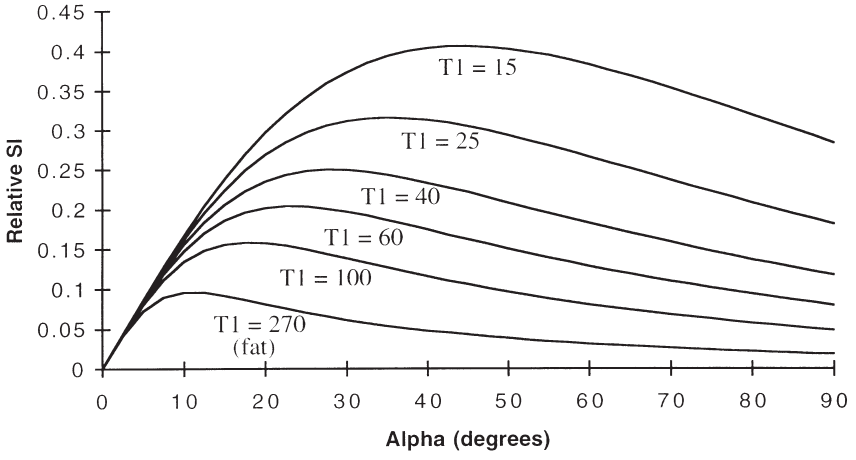

Figure 1. Relative signal intensity (SI) for different T1 values versus flip angle (a) for a spoiled gradient sequence. TR = 5 ms, TE <<T2*.

Gadolinium Chelates

At present, most CE-MRA examinations are conducted using gadolinium-based MR contrast agents. Gadolinium (Gd^{3+}) is a paramagnetic metal ion that decreases both the spin-lattice (T1) and spin-spin (T2) relaxation times.[23] Because Gd^{3+} itself is biologically toxic, it is chelated with ligands such as gadopentetate dimeglumine (DTPA), gadoteridol (HP-DO3A), or gadodiamide (DTPA-BMA) to form small-molecular-weight contrast agents.[24] These "extracellular" agents diffuse from the intravascular compartment into the interstitial space in a matter of minutes, meaning selective imaging of the vascular structures must be performed rapidly.[13,24] As compared with iodinated contrast agents, gadolinium chelates have a very low rate of adverse events and no nephrotoxicity, which is a significant advantage when evaluating patients with impaired renal function.[25-28]

Each gadolinium chelate decreases the T1 of blood according to the following equation[14,29]:

Equation #1

$$1/T1 = 1/1200 + R_1[Gd]$$

in which R_1 is the field-dependent T1 relaxivity of the gadolinium chelate, [Gd] is the concentration of gadolinium chelate, and *1200* (msec) is the T1 of blood without gadolinium (at 1.5 T).

A similar equation exists for T2, which is always shorter than T1.

Pulse Sequence

Dynamic CE-MRA exploits the transient shortening in blood T1 following intravenous (IV) administration of a contrast agent using a fast 3D spoiled gradient-echo sequence.[14,30,31] We use the term *transient* because this technique exploits the "first pass" of the contrast agent, as 80% of a typical gadolinium chelate leaks into the intravascular space within 5 minutes.[32] Typical repetition times (TR) for the 3D T1-weighted gradient-echo (SPGR, T1 fast-field echo [T1-FFE], or fast low-angle shot [FLASH]) sequence used for CE-MRA are less than 5 to 6 msec, with echo times (TE) of 1 to 2 msec and total scan times in the 10- to 30-sec range. This type of 3D sequence is ideally suited to MRA, as it has high spatial resolution and an intrinsically high signal-to-noise ratio (SNR). In addition, it is fast (can be performed in a breath-hold), and can be oriented and reformatted in any desired plane.[33-37] In addition, because intravascular signal is dependent on T1 relaxation, rather than on inflow or phase accumulation, in-plane saturation and turbulence-induced signal loss are not problems.[14]

The relative signal intensity (SI) for a 3D gradient-echo acquisition is given as[38]:

Equation # 2

$$SI = [N(H)\,(1 - e^{-TR/T1})/(1-\cos(\alpha)e^{-TR/T1})]\,\sin(\alpha)\,e^{-TE/T2^*}$$

in which $N(H)$, TR, TE, and α are the proton density, repetition time, echo time, and flip angle, respectively. As shown in Equation #2, SI is maximized when TR is long or T1 is short, since as (TR/T1) becomes large, $e^{-TR/T1}$ approaches zero. Of these options, shortening T1 is the primary method for increasing intravascular signal intensity, as lengthening TR and thereby increasing scan time is not desirable. The Ernst angle (α_E), which is important to understand to properly optimize parameters for a particular TR and expected T1, is defined as the flip angle maximizing the SI in Equation #2, and can be expressed as:

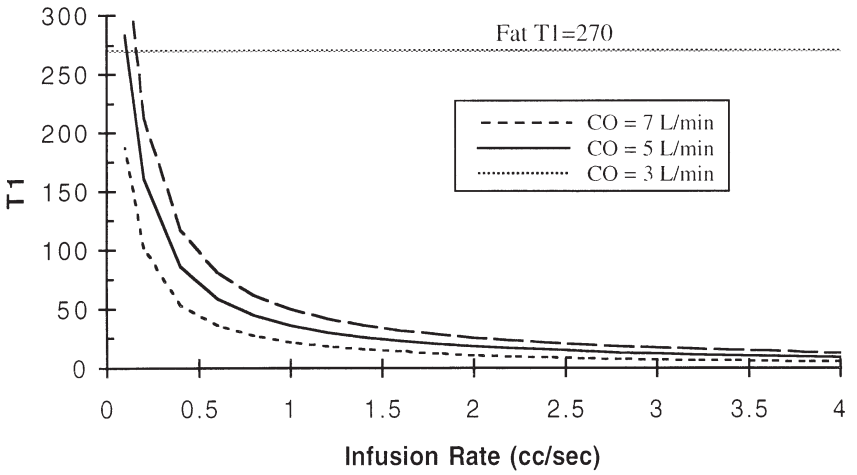

Figure 2. Blood T1 versus gadolinium infusion rate for changing cardiac output (CO), assuming no recirculation.

Equation #3

$$\alpha_E = \cos^{-1}(e^{-TR/T1})$$

Figure 1 shows an example of relative signal intensity versus flip angle α for different T1 values (assuming a TR of 5 msec with TE <<T2*). Note the significant increase in signal intensity as T1 approaches zero.

Contrast Dose and T1

In order for blood to appear bright with respect to background tissues during the arterial phase of dynamic 3D CE-MRA, sufficient contrast material must be administered to transiently reduce the arterial blood T1 to less than that of the brightest background tissue (ie, fat), which has a T1 of approximately 270 msec. During the first-pass arterial phase, blood T1 is more related to infusion rate and contrast agent relaxivity than to total contrast dose, as arterial phase imaging occurs well before intravascular contrast equilibration. This dynamic approach has the advantage of nearly eliminating steady-state background signal but at the same time (considering non–blood-pool agents) is essentially a "one-shot" technique, meaning that once contrast is administered and dynamic imaging performed, the process cannot be repeated without a second contrast bolus. If a second bolus is administered, not only are there the issues of expense and total patient dose, but residual soft-tissue enhancement can obscure vascular detail (as the biologic half-life of gadolinium chelates is approximately 90 minutes).[39] When using more than one injection, subtraction of a precontrast mask is desirable, and in some instances mandatory, for the second and third injections.[40]

Timing is extremely important in dynamic CE-MRA. In order to appreciate timing issues, the relationship among injection rate, blood T1, and resultant signal intensity must first be reviewed. For times shorter than the recirculation time, contrast concentration of the bolus in blood can be approximated as[13,14,41]:

Equation #4

$$[\text{Contrast}] = \frac{(\text{rate of contrast injection in mol/sec})}{(\text{cardiac output in L/sec})}$$

Although this simple equation ignores bolus dilution at leading and trailing edges, as well as extravasation of contrast in the lungs, a complex model originally developed for IV digi-

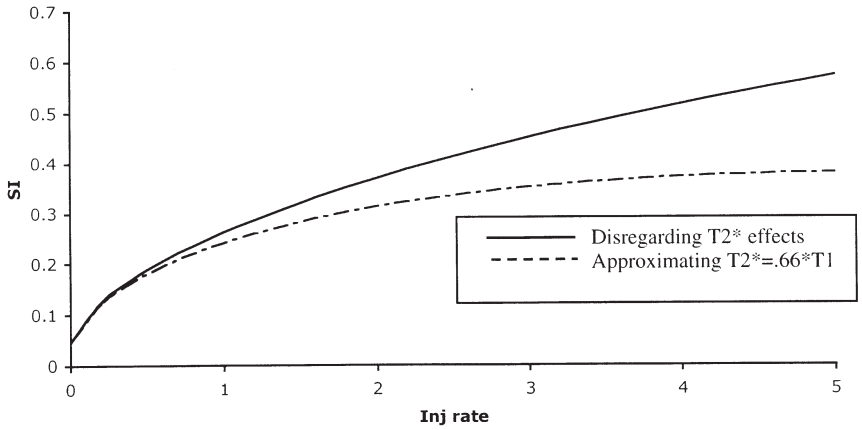

Figure 3. Relative signal intensity (SI) versus gadolinium injection rate for a spoiled gradient-echo sequence. Flip angle (α) = Ernst angle, cardiac output = 5 L/min.

tal subtraction angiography arrives at the same value for maximum contrast concentration.[42] Combining Equations #1, #2, and #4, and assuming no recirculation, blood T1 can be calculated for a given cardiac output and injection rate. This is demonstrated in Figure 2 for cardiac outputs of 3, 5, and 7 L/min using a standard gadolinium chelate preparation with a concentration of 0.5 mol/L.

Note in Figure 2 that for a "typical" cardiac output of 5 L/min, an injection rate of 1 mL/sec yields a blood T1 of 36 msec, while a 2 mL/sec injection gives a blood T1 of 18 msec. These T1 values are, in fact, much shorter than the T1 of fat, even though our own experience suggests true T1 values are not quite this short, being instead nearer double this estimate. Such a rapid injection rate, however, can, but need not necessarily, be sustained over the entire acquisition time. For a typical 80-kg patient receiving a "single dose" (0.1 mmol/kg) of gadolinium, this equates to 16 mL of a 0.5 mol/L gadolinium chelate preparation. Thus a 1-mL/sec injection can be sustained for 16 sec, or a 2-mL/sec injection sustained for 8 sec. Even though the acquisition time may be considerably greater than this, by properly timing the bolus with respect to image acquisition, as well as by realizing that a contrast bolus lengthens as it propagates from the venous to the arterial circulation, full advantage of the dynamic blood T1 shortening can be obtained. This is largely due to the unique way in which MR data are acquired.

Fourier (k-space) Considerations

MR imaging does not map spatial data linearly with respect to time as does conventional CT.[43] With 3D MR imaging, the entire 3D Fourier or k-space data set is collected before reconstructing individual slices. Because k-space maps spatial frequencies rather than spatial data, k-space data does not correspond to image space directly. Instead, different regions of k-space data determine different image features. For example, the center of k-space, or "low" spatial frequencies, dominate image contrast, whereas the periphery of k-space, or "high" spatial frequencies, contribute more to fine details such as edges.[44,45] This means that the state of the intravascular T1 in large vessels is essentially "captured" at the instant corresponding to acquisition of central k-space.[44] If central k-space is collected when arterial contrast concentration is peaking but has not yet reached the venous structures (arterial phase), only the arteries will enhance. The fact that intravascular contrast concentration may not be uniform over the entire acquisition time may generate artifacts, but these have been shown to be relatively minor provided that the contrast is not rapidly changing over the critical central portion of k-space and at least some "tail" of the contrast bolus is present during collection of high spatial frequency data at the periphery of k-space.[41,44] Thus with proper timing, gadolinium injection duration need not be as long as the entire acquisition time, and in fact many protocols use injection durations much shorter than the acquisition time with quite acceptable results.[46,47] For a given gadolinium dose, the injection strategy then becomes a trade-off between a fast injection (shorter T1—more intravascular signal) and long injection (more uniform T1—fewer artifacts). We have a general rule of thumb that advocates injecting the total contrast dose over a duration of approximately 50% to 60% of that of the acquisition for single station examinations.

Another factor that must be considered is phase-encoding order. Traditionally, phase encoding is performed "sequentially" so that central k-space is acquired at the mid-point of the scan. Alternatively, phase encoding can be performed in a "centric" fashion such that central k-space is acquired at the beginning of the scan.[48,49] Although centric phase-encoding order has been shown to be somewhat more prone to artifacts if the contrast concentration changes rapidly during acquisition of central k-space, it greatly simplifies bolus timing (which will be discussed below) and is less susceptible to artifact from incomplete breath-holds.[50,51]

CONTRAST MATERIAL INJECTION RATE

As shown in Figure 2, injection rates greater than approximately 2 mL/sec bring a diminishing return with respect to T1 shortening. But as shown in Figure 1, even small decreases in T1 lead to tremendous increases in signal intensity. By combining Equations #1 through #4, signal intensity (for TR = 5, TE = 2) can be plotted versus injection rate for a fixed cardiac output (5 L/min) and flip angle (Ernst angle) as shown in Figure 3. This is done both disregarding T2* effects, and using the approximation that T2* = (0.66)T1.[41]

This graph demonstrates that signal intensity increases asymptotically as injection rate increases, particularly when taking into account T2* effects, with negligible increases seen beyond a rate of 4 to 5 mL/sec.[52,53]

Different authors have taken different approaches to optimizing injection rate. Before the advent of high-speed gradient systems, which permitted total acquisition times of <1 minute (in the realm of a breath-hold), imaging times were on the order of 3 to 5 minutes, and injections were typically performed so that a "double dose" (0.2 mmol/kg) was administered at a uniform rate over the entire scan duration.[30,54] For a 4-minute scan on a 70-kg patient, this amounted to an injection rate of just over 0.1 mL/sec. With the much shorter acquisition times currently possible, many investigators advocate a double dose (0.2 mmol/kg, or alternatively a set volume of 20 or 30 mL) of gadolinium chelate with injection rates of 1 to 2 mL/sec. Others use up to a "quadruple dose" (0.4 mmol/kg) and rates of 4 to 5 mL/sec, while a new trend now advocates much smaller doses.[35,37,55-57] We personally believe that using a single 20-mL vial of gadolinium chelate with an injection rate of 1.5 to 2.5 mL/sec is generally a good compromise between maximizing arterial signal and minimizing artifacts for breath-hold scans.[58] Multi-station exams, large aneurysms or dissections, and cases in which venous evaluation is important are different, and these will be discussed shortly.

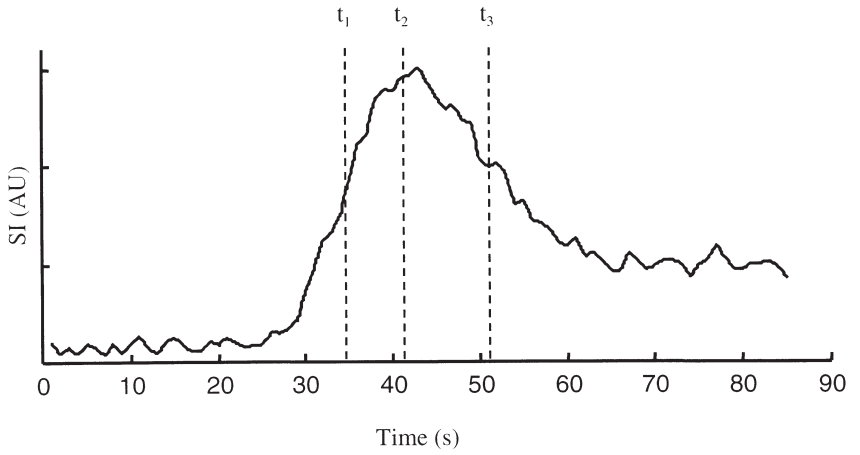

Figure 4. Relative signal intensity (SI) in the aorta versus time following a 9.5-mL injection of gadolinium chelate at a rate of 2 mL/sec.

CONTRAST-ENHANCED MRA: BOLUS TIMING CONSIDERATIONS

As discussed above, the timing of the Gd bolus acquisition of central k-space

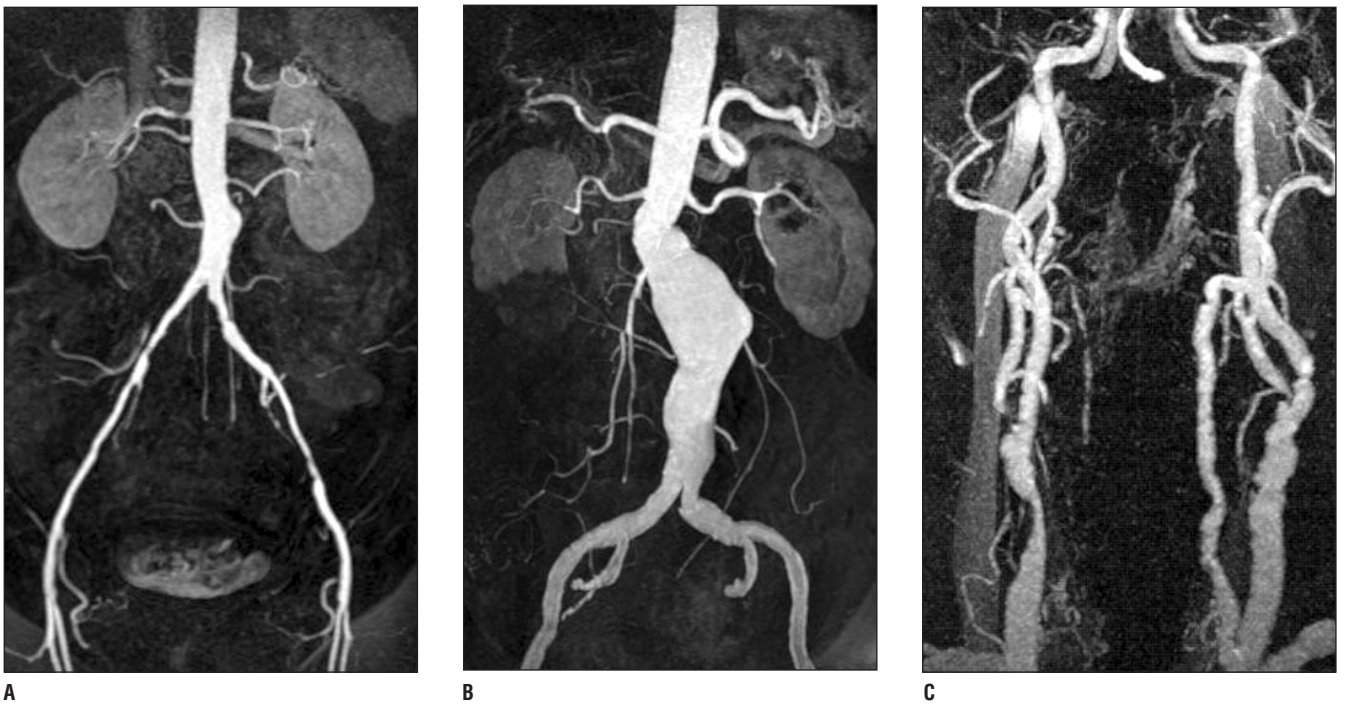

A B C

Figure 5. Maximum intensity projection (MIP) images from different MRA studies demonstrating: **(A)** good arterial phase timing in an abdominal aortic study, **(B)** slow flow through an abdominal aortic aneurysm with resultant leading edge artifact (mild ringing) and decreased signal-to-noise ratio (SNR) in the iliac arteries, and **(C)** a carotid MRA with slightly delayed triggering leading to mild to moderate enhancement of the right jugular vein.

is extremely important. The contrast travel time, defined as the time required for contrast to travel from the injection site to the vascular territory of interest, is highly variable, as is the degree to which the bolus "broadens" as it transits the heart and pulmonary circulation. A mean transit time to the abdominal aorta of 23 ± 5 sec, with a range of 13 to 37 sec has been reported.[59] An example of time resolved abdominal aortic SI (which is proportional to [Gd]) after IV injection of 9.5 mL gadolinium chelate at 2 mL/sec is shown in Figure 4.

As shown in Figure 4, note first that the arterial signal peaks relatively sharply (if the bolus were of longer duration, ie, larger total dose, the arterial peak would be somewhat lengthened). This observation has important implications. Because it has been shown that intravascular signal intensity is determined by the Gd concentration at the time the center of k-space is collected,[44] whether central k-space is acquired at time t_1, t_2, or t_3 (Figure 4) has a dramatic influence over the resultant image. Perfect timing (t_2) yields maximum arterial signal with minimal venous signal, as shown in Figure 5A. If, however, central k-space data is acquired too early (t_1—while arterial Gd is still increasing rapidly), "ringing" or "banding" artifacts of variable severity can be generated, as subtly demonstrated in the iliac arteries (Figure 5B).[44] These artifacts are also referred to as "leading-edge" artifacts since they result from imaging during the leading edge of bolus arrival. Acquiring central k-space data too late (t_3) leads to submaximal arterial signal intensity and associated venous enhancement. These two factors can be detrimental to evaluation of the arterial structures. A mild example of such delayed timing is shown in Figure 5C. Hence, if one knows, or can predict or measure the time course of intravascular Gd, the placement of central k-space can be tailored to achieve the desired image characteristics, be it maximum arterial signal, maximum portal venous signal, etc.

"Best-Guess" Technique

Several solutions to proper bolus timing have been offered. Perhaps the simplest solution is to just make an educated best guess. This involves estimating the contrast travel time from the site of injection to the vascular structure of interest. While this time is highly variable, an experienced MR angiographer can achieve good results reliably by taking factors such as injection site, age, cardiac output, and vascular anatomy into consideration. Sequential phase encoding is preferred when using a best guess, as this encoding strategy is more tolerant of timing errors (see the discussion of CE-MRA Logistic Considerations below).[44] Using this technique, timing can be calculated as follows[35]:

Equation #5

Imaging Delay = (Estimated Contrast Travel Time) + (Injection Time/2) – (Imaging Time/2)

where Imaging Delay is the delay between initiating the bolus and starting the scan (if negative, it refers to the delay between initiating the scan and starting the bolus). Equation #5 times the injection such that the mid-point of the bolus arrives at the desired vascular territory at the mid-point (center of k-space) of the scan. For example, a scan time of 18 sec with an estimated contrast travel time of 20 sec and a 20 mL gadolinium bolus at 2 mL/sec (10-sec injection), the imaging delay would be 20 + 10/2 – 18/2 = 16 sec (ie, start the acquisition 16 sec after initiating contrast injection). This timing is designed so the midpoint of the bolus arrives as the center of k-space is collected, meaning that depending on injection duration, there may already be venous enhancement by the time central k-space is collected. A potentially better timing strategy is:

Equation #6

Imaging Delay = (Estimated Contrast Travel Time) – (Imaging Time/2) + (Rise Time)

in which *Rise Time* is the expected time from arterial arrival to arterial peak, typically 3 to 5 sec. This timing formula places the center of k-space at the approximate peak of contrast concentration.

The most difficult aspect of the best-guess technique is estimating the contrast travel time. As previously alluded to, it is better to image slightly late (increased venous phase) than slightly early (ringing/banding artifact, Figure 5B). With this in mind, as a general guideline for travel time from an antecubital vein to the abdominal aorta, we start with approximately 15 sec for a young, healthy patient. A young hypertensive or athletic patient would require a few seconds less. A healthy, elderly patient would require approximately 20 to 25 sec. Patients with cardiac disease or an aortic aneurysm would be in the 25- to 35-sec range. Patients with severe cardiac failure in conjunction with aortic pathology might require up to 40 to 50 sec. We add 3 to 4 extra seconds if the IV line is in the hand.

Test-Bolus Technique

A better, and only slightly more time-consuming way to estimate contrast travel time is through use of a test bolus.[59-61] With this technique, 1 to 2 mL of gadolinium (followed by a 10- to 15-mL saline flush) is injected at the same rate as planned for the actual injection. Multiple single-slice fast-gradient-echo images of the appropriate vascular region are then obtained as rapidly as possible (at least every 1 to 2 sec) for approximately 1 minute. To minimize TOF effects, and thereby maximize contrast conspicuity, the 2D test bolus image should either be oriented along the vessel of interest (ie, sagittal or coronal for the aorta), or alternatively, be relatively thick (>1 cm) with a superior saturation band or a blood-nulling inversion pre-pulse. The time of peak arterial enhancement (contrast travel time) is then determined visually or by using a region-of-interest (ROI) analysis. Acquisition timing is then determined with Equation #6, keeping in mind that a longer bolus will take longer to peak

than a test bolus, and, therefore, a 3- to 4-sec Rise Time should be included. Alternatively, if centric encoding is desired (which is beneficial if the patient cannot breath-hold well[50]), the following equation should be used, again anticipating a Rise Time in the 3- to 4-sec range:

Equation #7

Imaging Delay = (Contrast Travel Time) + (Rise Time)

Using the test bolus technique for abdominal aortic imaging, Earls et al[59] demonstrated a mean aortic SNR increase of 902% (15 patients) following a 1-mL test bolus of gadopentetate dimeglumine. By utilizing the resultant contrast travel time (24.0 ± 12.6 sec), they were 100% successful in obtaining a "pure" arterial-phase study (as compared with 80% with best-guess timing), and saw significantly increased aortic SNR (29.8 versus 20.5).

There are three main drawbacks to the test-bolus technique. First, setting up, performing, and analyzing the test bolus lengthens the overall examination time. In experienced hands, the average time penalty reported was <5 minutes.[59] Second, the test bolus rapidly redistributes into the interstitial space, thereby increasing background signal. For such small test doses, however, these effects are negligible. Finally, there is no absolute guarantee that the imaging bolus will behave identically to the test bolus. This is because of moment-to-moment patient variables such as venous return and cardiac output, as well as the different total volume of injection. For example, a test bolus administered with the arm at the patient's side may not be accurate if the arms are above the head for the actual scan.

MR Fluoroscopy

A third method of contrast bolus timing uses extremely rapid "fluoroscopic" MR imaging.[45,62-64] With this technique, 2D sagittal gradient refocused images are rapidly (<1 sec/image) obtained through the vascular structure of interest, ideally using complex subtraction to improve the contrast-to-noise ratio and decrease artifacts. In this fashion, images are generated in near real-time and are updated at >1 image/sec. The operator can watch the contrast bolus arrive, then switch over to the centric 3D MRA sequence when the desired enhancement is detected.

This technique has the advantage of allowing real-time operator–dependent decision making. This may be particularly advantageous in the evaluation of cases with unusual or asymmetric flow patterns, such as unilateral stenoses and slow filling aneurysms. As an example, an abdominal aortic aneurysm can be monitored such that triggering is somewhat delayed in order to allow for complete enhancement of the iliac vessels, which may fill slowly (Figure 5B). The ability to assess the vasculature "on the fly" under these circumstances is a great asset, as is the time and contrast savings associated with not performing a test injection.

A recent refinement is to electronically shift the MR fluoroscopic monitoring to a proximal region of vascular anatomy to get more advance warning of contrast arrival.[65] Using carotid CE-MRA as an example, MR fluoroscopic monitoring in the chest shows contrast arriving in the subclavian vein, then right heart, pulmonary arteries, left heart, arch, and finally, proximal great vessels. Tracking the bolus over such a long period makes precise triggering easier. If the flow is very slow, the operator can compensate to allow for greater target vessel enhancement before triggering. This same work also demonstrates that fluoroscopic triggering is improved by recessing the absolute center of k-space a few seconds from the beginning of the 3D acquisition, thus avoiding early triggering, which can cause the previously described leading-edge artifact.

Temporally Resolved 3D Contrast MRA

Because proper bolus timing is so difficult and a timing mistake can ruin the study, some authors advocate "temporally" resolved techniques whereby multiple 3D datasets are acquired (or synthesized) extremely rapidly (typically 2 to 8 sec).[66-70] With such techniques, bolus timing is no longer a factor, as multiple vascular phases are obtained without any predetermined timing (ie, inject and begin scanning simultaneously). The operator simply selects the desired image set, be it pure arterial, maximum venous, etc. This is particularly useful in the carotid and pulmonary arteries, where the venous phase is extremely rapid, and in the case of vessels such as in the calf, where variable rate filling may occur due to stenoses, occlusions, or rapid arteriovenous shunting due to soft-tissue inflammatory disease.[66,70,71]

The most straightforward way to accelerate acquisition time is simply by scanning faster. This can be done using some combination of limiting the imaging volume, decreasing the resolution, decreasing TR, or using a parallel imaging technique, such as sensitivity encoding (SENSE).[72-75] Recent developments in gradient systems allow TRs of well under 2 msec on many systems, which is a three-fold improvement compared with just a couple years ago. In the pulmonary arteries, Goyen et al[73] achieved 4-sec temporal resolution using partial k-space filling (TR = 1.6 msec), although slice thickness was relatively thick at 5.5 mm reconstructed to 2.75 mm. In another approach, taken by Finn et al,[74] the aorta is imaged in two alternating planes (oblique sagittal and coronal, TR = 1.6 msec) at approximately 1 sec resolution per plane. This is in part possible due to a thick-slab acquisition (approximately 20 mm interpolated to 10 mm), meaning the data is quasi-projectional. While off-plane reformats in this case are poor, in-plane maximum intensity projections (MIPs) (two planes) are of high resolution. Finn et al has also used a 3D radial sampling scheme to further increase resolution.[76] Once high-resolution temporal data sets are obtained, even if the temporal resolution is insufficient for

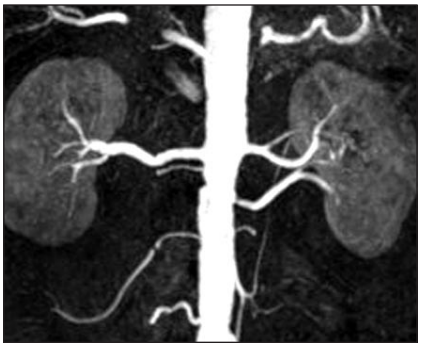

A

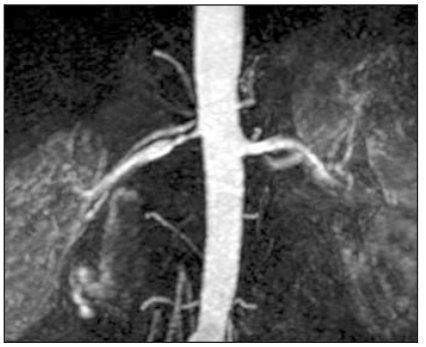

B

Figure 6. Coronal subvolume maximum intensity projections from renal MRA studies demonstrating (**A)** good breath-holding, and **(B)** poor breath-holding.

isolating the desired vascular phase, postprocessing techniques, such as correlation analysis can be used to synthesize images of a particular type, in this case pure pulmonary arterial versus pure pulmonary venous.[77]

Simultaneous high spatial resolution, high temporal resolution, and increased volume coverage can be obtained using the 3D time-resolved imaging of contrast kinetics (TRICKS) technique and its variants.[67,71,78-80] In the most basic implementation of this technique, k-space is divided into multiple blocks. The central block of k-space (which contributes most to overall image contrast) is collected repeatedly every 2 to 8 sec in an alternating fashion with the other blocks of more peripheral k-space. Images are then "synthesized" at high temporal resolution by piecing together each unique central block of k-space with a linear interpolation of the remaining k-space blocks acquired in closest temporal proximity. This technique allows greater temporal and spatial resolution/volume coverage than is available with a streamlined conventional sequence. The technique lends itself to "video" format, which allows passage of contrast material to be viewed directly. The 3D TRICKS-type sequences are now finding their way into commercial packages. The biggest drawback, other than the tremendously large number of images generated, is the large amount of processing time required to perform the multiple reconstructions, although this is rapidly improving. Also, k-space discontinuities, in conjunction with varying intravascular gadolinium concentration, can potentially lead to artifacts. These artifacts, however, have been shown to be small provided the gadolinium bolus is not too compact.[78]

A recent refinement in this strategy is to traverse k-space using radial or spiral projections, which allow for sliding window reconstructions at very high temporal and spatial resolutions.[81] One variation, known as vastly undersampled isotropic projection reconstruction (VIPR) is particularly promising.[82]

CONTRAST-ENHANCED MRA: LOGISTIC CONSIDERATIONS

The following logistic considerations apply to 3D contrast MRA in general, whether using best-guess timing, a test bolus, or triggering.

Artifacts: k-space–Related

As previously discussed, the key to maximizing arterial enhancement is to image such that the center of k-space is collected when arterial contrast concentration is at a maximum. Acquiring central k-space data after arterial contrast has peaked leads to suboptimal arterial signal and increased venous signal (Figures 4 and 5C). Acquiring central k-space during the rapid upslope in arterial contrast arrival causes "ringing"-type leading-edge artifacts (Figure 5B). Even with optimal timing, similar artifacts can be generated with the use of very compact boluses such that contrast falls rapidly while still acquiring relatively central k-space.[78] If the bolus is too short, such that the contrast concentration tapers too rapidly toward the end of the acquisition (high k-space frequencies), blurring of the edges results.[44] These artifacts are not as severe if k-space is mapped in a sequential, rather than a centric, manner.[44]

Thus, when using best-guess timing, sequential phase encoding is more forgiving. Also, if using this technique, we suggest slightly overestimating the contrast travel time so that the (inevitable) timing errors are more likely to cause increased venous enhancement than "ringing" artifacts. When using the test bolus technique such that contrast travel time is known, either centric or sequential phase encoding can be used. The advantage to centric phase encoding is twofold: less degradation with an incomplete breath-hold (see the discussion of respiratory artifacts below); and simplified operator logistics with respect to timing (no need to count backward to the middle of the scan to figure out when to inject; just inject, wait the proper delay, initiate breath-hold, and start imaging). For automated bolus detection, centric phase encoding is typically used. Because contrast rise times are not instantaneous, the delay from triggering to initiation of data acquisition becomes crucial in order to avoid artifacts. Examining Figure 4, if the 3D MRA triggers at time t_1, the appropriate delay is $(t_2 - t_1)$. This delay, of course, varies by patient and vascular territory. A delay of 3 to 6 sec typically works well for abdominal aortic imaging. In patients expected to have particularly slow flow (eg, in patients with congestive heart failure or an aneurysm), this time should be lengthened to 7 to 10 sec. In the carotid arter-

ies, however, which have a more rapid upslope and a very short arteriovenous window, shorter trigger delays of 2 to 3 sec are more appropriate in order to avoid jugular venous enhancement.[63,83] Recessing the absolute center of k-space from the beginning of the scan improves consistency by providing high arterial-phase contrast even if the trigger is premature.

Artifacts—Respiratory

Respiratory motion causes ghosting, blurring, and signal loss.[84,85] In 3D imaging, blurring occurs in the direction of the motion, whereas ghosting is most pronounced in the slow phase-encoding direction. For elliptical centric phase-encoding order, the ghosting is spread out in both phase-encoding directions.[86] Before the advent of fast imaging systems, 3D CE-MRA acquisition times were on the order of 3 minutes, making breath-holding an impossibility. Thus, early CE-MRA images suffered from significant image degradation, particularly when evaluating small vessels, such as renal arteries.[14] Figures 6A and B illustrate the difference between good- and poor-quality breath-holding.

There is no disagreement among researchers regarding the beneficial effects of breath-holding on abdominal and thoracic 3D CE-MRA.[35-37,50,87] Holland et al[87] evaluated the same 6 patients using both breath-hold and non–breath-hold renal 3D CE-MRA. They found that the non–breath-hold studies failed to identify 3 of 4 peripheral renal artery abnormalities, missed 1 of 2 accessory renal arteries, and were unable to visualize any of the renal artery bifurcations at the hilum. In contrast, breath-hold 3D CE-MRA identified all abnormalities, all accessory renal arteries, and renal artery bifurcations at the hilum in all patients. In the carotid arteries, breath-holding does not appear essential, although it does improve visualization of the arch vessels.[88]

Maki et al[50] looked at SNR loss and blur associated with incomplete breath-holds. Their work demonstrated that for typical MRA acquisition matrices and scan times, breath-holding during the acquisition of the central 50% of k-space was the most important for minimizing blur. This means that for centric phase encoding, the majority of the benefit from breath-holding can be obtained even if the patient begins breathing at the midpoint of the scan. Data from Wilman et al[51] shows that the more fully "centric" the phase-encoding order is, the less the artifact from partial breath-holds, and thus the preference for an elliptical versus a linear centric phase encoding order. These data suggest that for centric phase-encoding orders, an optimistic assessment of a patient's breath-hold ability is in order, as there is little to lose if they "don't quite make it." Recent data, however, has suggested that a large number of patients have a relatively large degree of diaphragmatic motion even during an apparently successful breath-hold.[86] This causes blurring and ringing artifacts within the visceral arteries, obscuring small vessels and subtle abnormalities (such as those that occur with fibromuscular dysplasia), in effect counteracting the spatial resolution inherent in the sequence. This argues for shortening abdominal MRA acquisition times to well below potential breath-hold times, making rapid acquisition techniques, such as SENSE and the ultra-short TR discussed above, even more attractive. In anatomic regions that can remain truly motionless, such as the calves and feet, long acquisitions work well.[47]

We have found that patients are better able to breath-hold if the procedure and expectations are described well in advance of the actual scan. The vast majority of ambulatory patients can breath-hold for at least 20 to 30 sec, while many have endurance well beyond this. While performing a test breath-hold before the scan is always a good idea, watching a patient's respiratory pattern often gives you a clue to their breath-hold potential. In our experience, patients who take slow deep breaths with relatively long expiratory pauses have no problem completing a 30- to 40-sec breath-hold. Patients who breath rapidly (>25 breaths per minute) with no pause between expiration and subsequent inspiration often have trouble with a breath-hold of this duration. Sick or postoperative inpatients often cannot, or will not, hold their breath at all, again making the high temporal resolution scanning more attractive.

We recommend the following breathing strategy. For best-guess or test-dose bolus timing techniques, pre-breathe the patient for 3 or 4 cycles (saying, "deep breath in... and breath out...") timed so that the last inspiration is held ("deep breath in and hold...") as the scan starts. Some authors advocate the use of supplemental oxygen during this pre-breathing.[35,86] For fluoroscopic techniques, pre-breathe the patient 3 or 4 cycles, then have them relax, start the fluoroscopic sequence, and wait for bolus arrival. Once the MRA sequence is triggered, use some pre-arranged signal, such as squeezing the patient's arm in addition to a loud verbal "hold your breath" to initiate the breath-hold. This needs to occur during the delay time, so that the patient is motionless once the actual data collection starts and the critical center of k-space is collected.

Determining Imaging Time

The duration of a 3D CE -MRA acquisition (t_s) depends on several variables, and can be approximated as:

Equation #8

$$t_s \sim TR * YRES * ZRES * (\text{fractional y FOV})/(SF)$$

in which TR is the repetition time, YRES and ZRES are the number of phase-encoding steps in y and z, fractional y FOV is the asymmetric y field-of-view fraction, and *SF* is the speedup factor due to parallel imaging techniques, such as SENSE.[89] Repetition time is itself a function of echo time (TE), echo type (ie, full or fractional),

and bandwidth. Spatial resolution is determined by voxel size, which is determined by the following equation:

Equation #9

voxel size = (y FOV/YRES) by (z FOV/ZRES) by (x FOV/XRES)

in which *x*, *y*, and *z* FOV refer to the x, y, and z fields of view, and XRES is the number of data points digitized during readout. Using fractional y field-of-view decreases the number of y phase encodings, shortening scan time while maintaining resolution but collecting a smaller (or "rectangular") FOV in the y direction. This is particularly useful for large FOV studies where structures at the periphery of the y FOV are not important, and wrap around (aliasing) can be tolerated. Parallel imaging techniques, such as SENSE, require the use of multiple (phased-array) coils. These techniques collect fewer phase encodings than are prescribed (phase and/or slice direction), effectively reducing the FOV(s) with resultant aliasing.[75,89,90] This can decrease scan time by up to a factor of the number of coils in the phased array, depending on geometry. SENSE has, to date, been most useful for cardiac imaging, although it appears to have great potential with MRA as well.[91,92] Using sensitivity data for each phased-array coil obtained from a quick "reference" scan, a mathematical algorithm can then "unfold" the aliased data set, restoring the original prescribed FOV with only a small geometry-related loss in SNR when coils are properly optimized. One important concept to remember when using SENSE is that the prescribed FOV must be such that there is no aliasing, or else the reconstruction algorithm breaks down and causes severe aliasing artifacts. Thus, SENSE is most advantageous when a full rectangular FOV is desired.

All of these parameters must be juggled to achieve the required volume coverage, spatial resolution, and SNR while keeping the scan time (t_s) within an acceptable range, which should be as short as possible and certainly within the patient's anticipated breath-hold duration (t_b). Thus, there are multiple trade-offs. Increasing resolution (YRES or ZRES with same overall slab thickness), increasing volume coverage (ZRES with same slice thickness), or increasing SNR (decreasing bandwidth or changing from fractional to full echo), all increase t_s. Decreasing the rectangular FOV or using a parallel imaging technique will decrease t_s. The SNR must also be considered. In general, for all these techniques, SNR scales as the voxel size times the square root of scan time t_s.[38,41] One interesting property unique to contrast MRA, however, is that all other things being equal (eg, not changing bandwidth), if the contrast injection rate is increased proportionally with the decrease in scan duration (ie, inject same total contrast dose faster), the SNR is unchanged and CNR increases. Maki et al[41] describe a mathematical analysis specific to breath-hold CE-MRA to optimize SNR by considering these variables.

A useful technique with no associated time penalty is to zero-fill k-space in multiple directions.[93] Most MR scanners have an option to zero-fill both frequency and phase to 256 or 512. In addition, a 2x zero-fill in slice can be specified, yielding twice the number of slices. While the slice thickness is unchanged, the slices now overlap by one-half a slice thickness. While zero filling may not increase resolution, it permits smoother reformats by reducing partial volume effects.

The art, then, of 3D breath-hold CE-MRA boils down to a careful choice of the parameters in Equations #8 and #9 and is often an iterative process. As a general rule for non–time-resolved abdominal MRA, we start with a frequency resolution (XRES) of approximately 400, with zero-filling to 512 × 512 in frequency and phase, and times 2 in slice. We then consider the maximum estimated breath-hold duration (t_b) and desired slice thickness. We increase ZRES to cover the required volume. If an asymmetric FOV can be used, we do so. Alternatively, we use SENSE with a SF of 2 to 3.[47,89] We then increase YRES until t_b is reached. Always keep in mind the voxel dimension in z versus that in y. They should be roughly similar, as one fundamental purpose of a 3D data set is to generate relatively isotropic resolution so that multiplaner reformats (MPRs) maintain resolution in all planes.

If t_s cannot be made less than t_b after these manipulations, then sacrifices must be made. Partial Fourier techniques can be used (ie, collect only a fraction of y phase encodes) at the cost of a decreased SNR. Alternatively, bandwidth can be increased, again at the cost of a decreased SNR, or slice thickness can be increased at the cost of decreased spatial resolution. Higher SENSE factors (>2.5 to 3.0) can be employed, although this also decreases SNR. Finally, incomplete breath-holding can be anticipated at the cost of increased ghosting and blurring.

In cases where breath-holding is not as important, such as in the extremities or carotids, there is more flexibility with regard to choosing imaging parameters. In these circumstances, the limiting factor becomes contrast bolus duration. As previously described, a "compact" bolus (with respect to imaging duration) can cause artifacts such as ringing and blurring. So, assuming a double dose (0.2 mmol/kg) of a gadolinium chelate (0.5 mol/L) for a 80-kg patient administered at 2 mL/sec, the injection duration is only 16 sec. Assuming the bolus will broaden by several seconds before reaching the target vessels, this is still less than approximately 20 to 22 sec. To avoid artifacts, this needs to be a substantial fraction of the scan time t_s, and scan times much greater than approximately 60 sec are likely counterproductive. Nonetheless, this increase in imaging time allows for increased SNR and spatial resolution. When considering carotids or peripheral vessels with soft-tissue disease, the rapidity of venous return must also be considered. This limits scan duration, as the longer

the scan, the closer the proximity of phase encoding to central k-space when venous signal arrives. This leads to greater venous signal and leading-edge venous ringing artifact. With truly centric sequences, however, carotid scan times of up to 40 sec and lower station peripheral scan times of well over 1 minute have been shown to work extremely well, in part due to recirculation of contrast in the latter part of the scan.[47,63]

Patient Preparation

The more relaxed and informed a patient is, the more easily they can remain still and perform a long breath-hold. Therefore, reassurance and a brief description of the scan can really help. In patients who are particularly anxious, premedication with sedatives, such as diazepam, may be useful. This helps the patient to relax and lie still, and also decreases cardiac output.[14] This latter effect helps enhance image quality, as arterial phase [Gd] increases with decreasing cardiac output (Equation #4) (Figure 2).

Since most 3D CE-MRA is performed in the coronal plane, arm position is important to allow for a smaller FOV without aliasing, particularly if using SENSE. For carotid, large FOV aortic, or peripheral studies, the arms can remain by the patient's side, as aliasing is not a factor. For pulmonary, small FOV aortic, renal, and mesenteric studies, the arms must either be elevated out of the imaging plane using cushions, or extended over the head.[35] Both of these positions in which the arms are elevated have the added benefit of gravity-aided venous return from the IV injection site.

We recommend placing the IV before the patient is in the magnet. This alleviates anxiety and possible shifts in patient position that may occur if it is placed while in the magnet. If the MRA is performed with the arms by the patient's side, placing the IV in the antecubital vein is adequate. If the arms are positioned over the head, it is preferable to place the IV below the antecubital fossa so it will not kink and obstruct should the patient's elbow bend. A 22-gauge catheter is usually adequate, although for smaller diameter catheters (>22-gauge), warming the contrast to body temperature may decrease the viscosity enough to allow for adequate injection rates.

Contrast Injection

As previously described, the total Gd dose and rate of delivery is a trade-off between maximizing intravascular signal and minimizing artifacts. In the ideal situation, a large dose at a high rate would be optimal. This, however, must be weighed against safety, practicality, and cost. We feel that for breath-hold CE-MRA with accurate bolus timing (test bolus or fluoroscopy), a single dose (0.1 mmol/kg) administered at a rate of approximately 1.5 to 2 mL/sec represents a good balance between these factors, depending on total scan time. In practice, however, once a bottle (typically 20 mL) of gadolinium is opened, it is best to inject the entire bottle, and hence we typically use 20 mL. For best-guess techniques, we prefer closer to 0.2 mmol/kg (eg, 40 mL) at the same approximate rate. These recommendations can, under certain circumstances, be modified. For example, in a particularly small patient for whom the volume of a single dose is small, artifact from a compact bolus may be generated. To remedy this, either the injection rate can be decreased (thereby lengthening the bolus at the expense of intravascular signal), or the dose can be increased (at the expense of increased cost). If cost is an overwhelming concern, the dose and injection rate can be decreased at the expense of intravascular signal, or the dose alone can be decreased at the risk of compact bolus artifact.

In experienced hands, we find that manual contrast injection works quite well. Since many smaller MR centers do not have a power injector, this is often the only choice. Manual injections are also simpler in some ways, as there is less "plumbing" and less opportunity for mechanical difficulties. A power injector, however, offers a more constant and standardized bolus delivery. Either way, the contrast injection must be followed rapidly by adequate saline flush to complete delivery of the bolus and help flush the arm veins. Suggested flush volumes range from 15 to 50 mL, while most authors report using 15 to 20 mL.[35,59] We suggest 25 mL of saline flush at the same rate as the Gd bolus. For hand injections, a standardized tubing set that allows rapid switch-over between Gd and saline injection works well (Smartset, TopSpins, Plymouth, MI).

Imaging Different Vascular Phases

With most 3D CE-MRA studies, extensive efforts are made to image the arterial phase optimally, as has been discussed extensively. Once the arterial phase data set is collected, however, the sequence can (and should) be repeated to obtain venous and equilibrium phases. Later phases are useful in evaluating unsuspected dissections, portal venous or venous structures, parenchymal enhancement patterns, and perhaps even renal glomerular function.[94,95] Temporal resolution is determined by a combination of scan time and the time required for the patient to prepare for another breath-hold. Aside from techniques such as 3D TRICKS, the faster the scan, the better the potential temporal resolution.[67] In cases in which high temporal resolution is desired (such as in the carotids or in cases of arteriovenous shunts), the previously described streamlined techniques can be used in a single breath-hold, although SNR and spatial resolution decrease.[66] In more conventional breath-hold 3D CE-MRA, with a scan time of approximately 20 to 25 sec, we advocate giving the patient approximately 8 to 10 sec to "catch their breath," then scanning again. In this manner, the second arteriovenous phase occurs approximately

35 sec after peak arterial phase. This is usually well timed for the portal venous phase, and often adequate for evaluating venous structures and parenchymal phases in the visceral organs. Sometimes, a third phase may be desired, usually to evaluate slow venous return or the renal collecting system.

Because these later phase examinations occur more in the equilibrium phase of Gd distribution, intravascular T1 is increased, and therefore signal is reduced as compared with the arterial phase (Figure 5C). In order to maximize signal in these later phases, the flip angle should, if possible, be reduced (Figure 1). While the optimum flip angle for the arterial phase may be 30° to 40° at a TR of 4 to 6 msec, the optimal flip angle decreases to 15° to 25° in later phases. To image Gd excreted into the collecting system and ureter, use a high flip angle (45° to 60°) with the widest bandwidth and shortest possible echo time.

Postproccessing and Display

Three-dimensional CE-MRA produces a contiguous volume of image data. For a typical body MRA study, this volume is asymmetric, perhaps $400 \times 300 \times 64$ mm. For a representative acquisition matrix size of $400 \times 150 \times 32$, this yields a true voxel size of $1.0 \times 2.0 \times 2.0$ mm. For diagnostic purposes, this data set is best viewed interactively using a computer workstation allowing for thin multiplanar reformation (MPR).[1,58] In this manner, thin (1.0 to 2.0 mm in this case) slices can be viewed in axial, sagittal, coronal, or oblique planes, thus eliminating overlapping structures and unfolding tortuous vessels. Because these reformatted slices remain thin and are not projections (see below), they not only provide the best achievable contrast, but also minimize the chance of diagnostic error.[1,58,96]

Because thin reformations show only short vascular segments, it is advantageous to utilize the MIP postprocessing technique.[97,98] Using this algorithm, the user first specifies the subvolume thickness and desired viewing plane. The algorithm then generates rays perpendicular to the viewing plane, takes the maximum value of any voxel encountered along that ray, and assigns that maximum value to the corresponding pixel in the output image. This technique is fast, and works extremely well with techniques such as CE-MRA, since vascular signal is typically much greater than background signal. It provides projection images that are quite similar in appearance to conventional angiograms. The MIP algorithm is demonstrated in Figure 7, which shows a full thickness coronal MIP of the thoracic aorta (Figure 7A), a thin-slice axial reformation through the aorta at the level of the pulmonary arteries (Figure 7B), and an oblique subvolume MIP taken from the axial reformat demonstrating the origins of the great vessels and a large Stanford B aortic dissection (Figure 7C). As can be seen, this technique is very helpful for displaying complex vascular anatomy, particularly when vessels are not oriented along a single plane.

Despite its usefulness, the MIP algorithm is subject to artifacts. Perhaps the most common artifact arises when stationary tissue has greater signal intensity than the vascular structures of

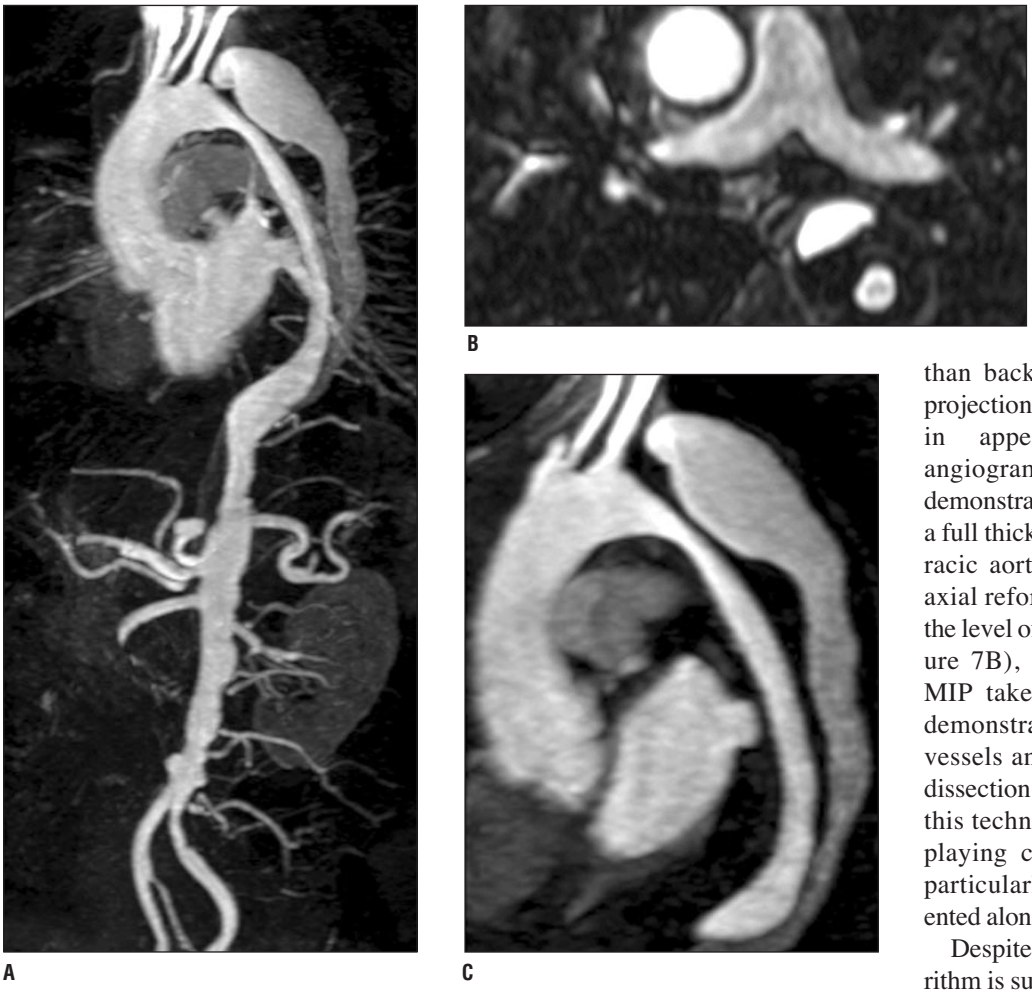

Figure 7. Stanford type-B aortic dissection. **(A)** Full-volume oblique sagittal maximum intensity projections (MIP). Note the bovine arch. **(B)** Axial multiplanar reformat showing the two lumens with mural thrombus in the false lumen. **(C)** Subvolume MIP demonstrating the intimal flap with paired true and false lumens.

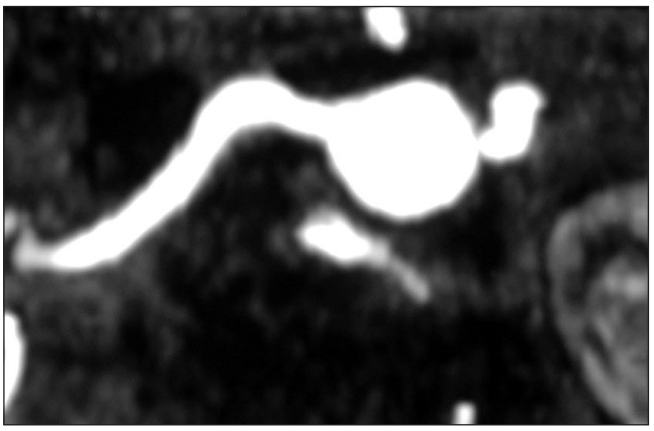

A

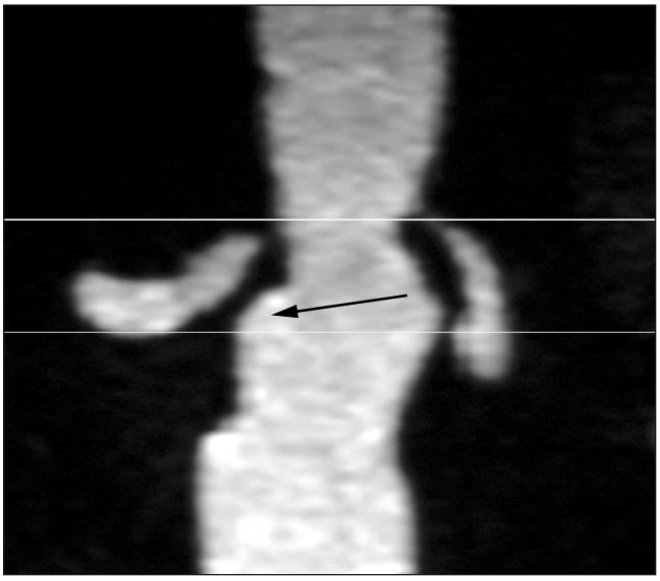

B

Figure 8. Demonstration of a potential maximum intensity projection (MIP) artifact. **(A)** Subvolume axial MIP through the right renal artery looks normal. **(B)** Careful review of the source coronal images demonstrates how the MIP volume (white lines) incorporates part of the ectatic aorta (black arrow), masking the high-grade right renal artery stenosis.

interest, as can occur in the presence of other vessel segments, fat, hemorrhage, metallic susceptibility artifacts, or motion artifacts. This, in turn, leads to the mapping of nonvascular signal into the projection image and causes a discontinuity in vessel signal, potentially mimicking a stenosis or occlusion (Figures 8A and B).[1] This type of artifact is best overcome by minimizing the thickness of the MIP subvolume, thereby excluding as much extraneous data as possible. Other artifacts inherent to the MIP technique have been described.[99] These mainly consist of underestimating vessel lumen, and are more of a problem with TOF or phase-contrast techniques. Because of these potential pitfalls, most authors agree that the MIP images should be used as a roadmap, utilizing the source images for definitive diagnosis.[1,58,99] A new study suggests that volume rendering is more accurate than the MIP and is similar to using MPR, but should still not replace careful evaluation of the source images and MPRs.[100]

Subtraction techniques are also useful in image evaluation, particularly in vascular regions not subjected to significant respiratory motion. These areas include the extremities, pelvis, and carotids. A digital subtraction MRA can be accomplished most easily by subtracting precontrast from postcontrast magnitude (reconstructed) images. Provided the patient maintains the same position on both studies, subtraction will eliminate background signal and improve vessel conspicuity. This technique has been used successfully in the extremities.[40,101] An improvement on this technique, particularly for thicker-slice or 2D examinations, involves complex subtraction of the precontrast and postcontrast "raw" (k-space) datasets. This overcomes phase differences in voxels that contain both stationary and moving spins (ie, very small vessels), allowing for increased vascular signal.[102,103]

CONTRAST-ENHANCED MRA: CLINICAL APPLICATIONS

This section reviews techniques and imaging parameters for selective body CE-MRA studies. The parameters provided here were largely derived from clinical experience with the Philips Intera 1.5-T system (Philips Medical Systems, Bothell, WA). The general techniques described here are easily applicable to other systems, although the parameters may need to be extrapolated as appropriate.

Based on the previous discussion, several general principles apply when performing CE-MRA. First, TR and TE need to be as short as practical without excessively increasing the bandwidth. Echo time can, and should, be minimized using a partial (asymmetric) echo. For the Intera system using an XRES of 400 with a water-fat shift of approximately 0.8 (bandwidth of ± 36.8 kHz), minimum TR/TEs of approximately 4.0 to 5.0/1.2 to 2.0 msec are possible (somewhat dependant on choice of coil). Some systems are capable of even shorter TRs, although because SNR decreases as the square root of bandwidth, care should be taken not to increase bandwidth excessively to achieve minimal decreases in TR. Second, phase (y) and slice (z) resolution should be relatively balanced and ideally no greater than approximately one-third the smallest vessel of interest.[104,105] In general, most MRA practitioners tend to let the z resolution (slice thickness) drift somewhat lower than the phase (y) resolution. Note that the resolution in the frequency (x) direction is typically somewhat greater than in the phase and slice directions. For most abdominal applications, y and z resolutions of 1.8 to 2.4 mm are adequate, although for

A

B

Figure 9. (A) Coronal maximum intensity projection from an abdominal aortic MRA demonstrating a focal infrarenal dissection. **(B)** Coronal source image showing the site of intimal disruption.

imaging large structures, such as the portal vein or thoracic aorta, where fine detail is not of great concern, increasing resolution to 2.5 to 3.0 mm is often acceptable,[106] and for vessels, such as peripheral below-the-knee vessels or carotids, isotropic resolutions of 1.0 mm are appropriate.[47,107] Third, to benefit from breath-holding, which is essential in the abdomen, the number of slices and phase-encoding steps must be balanced between adequate volume coverage, adequate resolution, and estimated breath-hold time. For a typical field-of-view of 400 × 300 mm, 192 phase encodings corresponds to a y resolution of 2.1 mm. For 192 phase encodings and a TR of 5 msec, approximately 35 slices can be obtained in a 25-sec breath-hold. These imaging times can be further reduced using partial Fourier imaging (halfscan, 1/2 number of excitations) or SENSE. For example, a SENSE factor of 2.5 with an FOV of 400 × 400 and the same TR and YRES, the same volume could be obtained in just over 13 sec. Alternatively, 65 slices could be obtained instead of 35 in the same 25 sec. Finally, for most arterial phase studies, it is best to use an automated bolus detection technique. This is particularly important for renal and carotid studies, where delayed timing causes artifacts due to adjacent venous opacification. If automated bolus detection is not available, a test bolus can be used. If neither of these techniques is feasible, educated best-guess timing can be used as a fallback.

Abdominal Aorta/Iliac Arteries

Three-dimensional CE-MRA of the abdominal aorta and iliac arteries is most often performed to evaluate aneurysmal disease (Figures 5A and B), dissection (Figure 9), or as part of a claudication work-up. The acquisition is performed in the coronal plane to facilitate evaluation of the iliac and renal vessels, and a phased-array body coil should be used whenever possible. The imaging volume can be prescribed from a breath-hold sagittal 2D black-blood gradient-echo or true fast imaging with steady state precession (true FISP) "bright blood" localizer, or alternatively from an MIP reformat of a fast low-resolution axial 2D TOF sequence. A breath-hold localizer is preferred, as it captures the anatomy in the same position in which the CE-MRA will be performed, thus decreasing the chances of a vital structure (such as the anterior aspect of an aneurysm) falling outside the FOV. It also gives the patient a chance to practice a breath-hold when the outcome is not crucial.

A 400 × 300 mm FOV with a 400 matrix and y resolution of approximately 2 mm is a good starting point for CE-MRA of the abdominal aorta (approximately 400 × 200 matrix). If the patient is large or has iliac/thoracic aortic disease, the FOV and slice thickness can be increased as needed. As previously described, slice thickness and number of slices are chosen based on desired resolution and breath-holding capability. Ideally, true slice thickness should be approximately ≤2.4 mm. For very large aneurysms, however, it may be necessary to increase slice thickness to 3 or 4 mm. Breath-holding is important for aorto-iliac evaluation, particularly if good evaluation of the renal arteries is desired. Often, however, surprisingly good aortic and iliac image quality can be obtained even for patients who breath-hold poorly.

Because large aneurysms have a slow, swirling flow, extra time is required for the aneurysm to opacify maximally and to allow for filling of the iliac arteries (Figure 5B). When using fluoroscopic bolus detection, we find it useful to trigger approximately 2 to 3 sec beyond where we normally would (assuming a flouroscopy to 3D CE-MRA delay of 3 to 4 sec). With a large aneurysm or known dissection, we typically use a full 40 mL of Gd; otherwise, 20 mL works well. Obtaining a delayed-phase image immediately following the arterial phase is recommended, particularly for dissections or very-slow-filling aneurysms.[70]

Thoracic Aorta

As with the abdominal aorta, thoracic aortic MRA is most often performed for aneurysm or dissection (Figures 7 and 10). When evaluating the thoracic

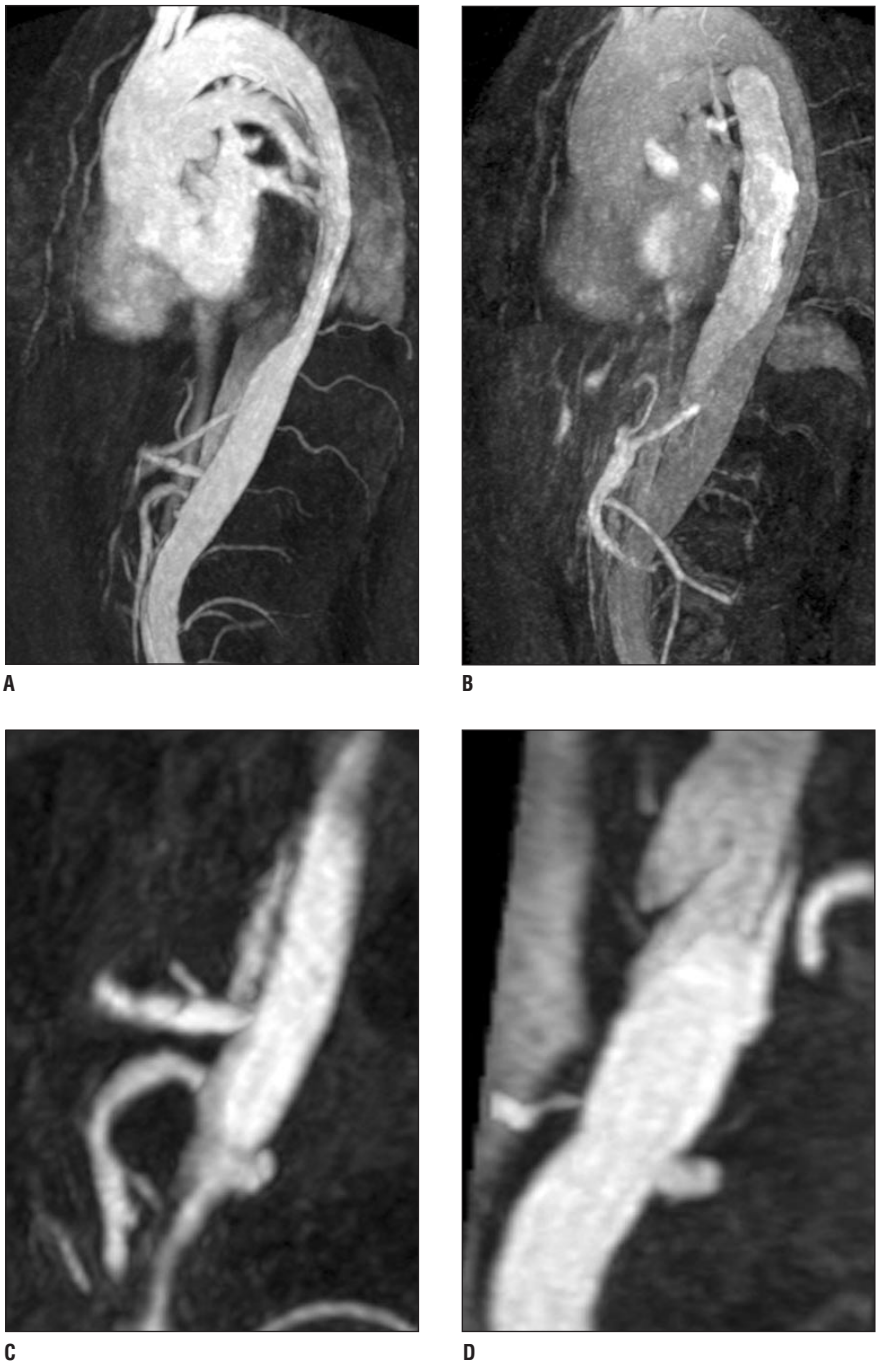

Figure 10. (A) Arterial and **(B)** immediate delayed phase full-volume maximum intensity projections (MIPs) from a thoraco-abdominal MRA. The more posterior false lumen opacifies more rapidly and extends into the iliac arteries, with the delayed phase better demonstrating the more anterior true lumen. **(C)** Sagittal and **(D)** coronal arterial phase subvolume MIPs help define the extremely complicated anatomy in this case. A stenotic right renal artery and superior mesenteric artery originate from the true lumen, whereas the celiac axis and a proximally occluded left renal artery originate from the false lumen.

aorta, an oblique sagittal 3D volume oriented with the arch typically works best, minimizing the total number of slices. Obtaining two dynamic phases is extremely important, particularly with dissections, where slow-filling lumens may opacify much better on the venous phase (Figures 10A and B). We typically use 40 mL of Gd in the presence of a known dissection.

When targeting only the thoracic aorta, a phased-array body coil and an FOV of approximately 380 × 266 mm should be used, as a moderate amount of aliasing can be tolerated. When evaluating the entire thoraco-abdominal aorta, the built-in body coil is typically used, as most phased-array coils do not have sufficient craniocaudal coverage. Using an FOV of approximately 440 × 290 mm, the entire aorta to the bifurcation can usually be covered, including the renal artery origins (Figure 10D). In either case, the origins of the great vessels should be included in the imaging volume. True slice thickness can be as great as 3 mm, although if renal artery evaluation is important, thinner slices (approximately 2.4 mm) are desirable. Total number of true slices depends on the size and tortuosity of the aorta, as well as slice thickness, but is typically in the range of 30 to 40.

A complete evaluation of the thoracic aorta includes multiplanar cardiac-gated black-blood imaging of the aortic wall to detect intramural hematoma, an important prognostic indicator,[108] although a complete description of this is beyond the scope of this review.

Renal Arteries

Contrast-enhanced MRA of the renal arteries is similar to an abdominal aortic study, with the exception that including the entire iliac vasculature is less important (although useful, if possible). This allows for a thinner coronal slab, and therefore decreased slice thickness and/or acquisition time. Typically, approximately 30 slices with a true slice thickness no greater than 2.2 to 2.4 mm, a matrix of 400 × 230, and an FOV of 400 × 300 mm is sufficient. This allows for high resolution (1 × 1.7 × 2.2 mm) with relatively short scan times (under 20 to 25 sec). As discussed previously, breath-holding is extremely critical, as distal branches and accessory renal arteries are diffi-

A

B

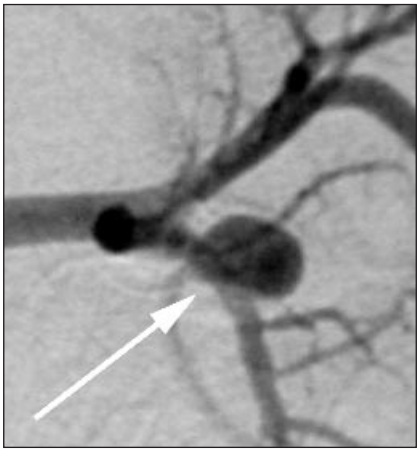

C

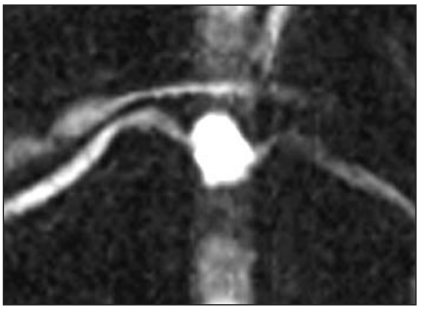

D

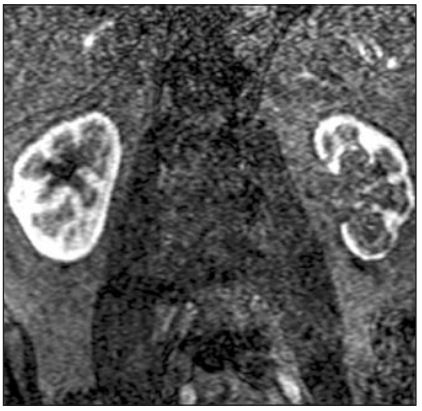

E

Figure 11. (A) Full-volume maximum intensity projection (MIP) from a renal artery study with angiographic correlation **(B and C)** demonstrating high-grade left, and moderate- to high-grade right renal artery stensosis, as well as a small left renal artery aneurysm (arrows). **(D)** Axial MIP from a phase-contrast study demonstrates no signal drop-out on the right, with mild signal drop-out on the left, indicating probable hemodynamic significance of the left renal artery stensosis. **(E)** Examining the source images can provide addition clues to the hemodynamic significance of a lesion, as in this case where smooth left renal cortical thinning is seen.

cult to evaluate in the presence of diaphragmatic motion.[86] This and other recent studies suggest that minimizing acquisition time (and thereby motion artifacts) is extremely beneficial. Techniques as simple as limiting the volume coverage or as advanced as SENSE are good choices for the renal arteries.[91]

Figure 11 demonstrates a mild to moderate right stenosis and a moderate to severe proximal left renal artery stenosis (Figure 11A), with angiographic correlation (Figures 11B and C). Note that 3D phase-contrast imaging (Figure 11D) can be a useful adjunct in the evaluation of renal artery stenosis. While the CE-MRA images demonstrate anatomy, the PC images show signal loss in regions of turbulence or extremely slow flow, suggesting which lesions are of hemodynamic significance.[109,110] In this example, there is no right-sided signal loss, but moderate signal drop-out on the left, suggesting the left-sided lesion is hemodynamically significant, which was confirmed by X-ray angiography (Figure 11B). Note also the left-sided cortical thinning (Figure 11E), a secondary sign of significant renal artery stenosis, as well as the incidentally noted small left renal artery aneurysm (Figure 11A), which was nicely corroborated on a later phase X-ray angiogram (Figure 11C). Figures 12A and 12B demonstrate an MIP and a volume-rendered image from a patient with proven fibromuscular dysplasia.

Transplant renal arteries can be evaluated easily as well.[111,112] An example is shown in Figure 13, in which the transplant artery has thrombosed with subsequent infarction of the renal graft. Since transplants are in the pelvis, respiratory motion is not as problematic, and breath-holding is less critical. Nonetheless, it is best to have the patient breath-hold if possible. While coronal imaging with a 320- to 360-mm FOV is usually adequate, oblique sagittal imaging can be performed with a smaller FOV. This gives higher resolution, but covers much less vascular territory. Transplant renal veins are easily seen on the venous phase of the study.

Mesenteric Arteries

The proximal mesenteric vessels are included on renal or abdominal aortic CE-MRA studies, and are usually well visualized, even in the presence of respiratory motion (Figure 14). The inferior mesenteric artery is often seen as well.

Dedicated mesenteric artery studies, typically for the evaluation of mesen-

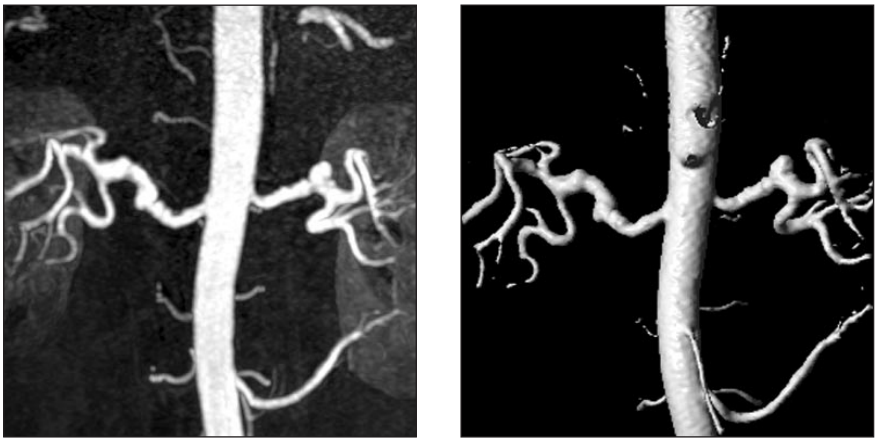

A B

Figure 12. (A) Maximum intensity projection and **(B)** volume-rendered image from a renal MRA in a patient with proven fibromuscular dysplasia.

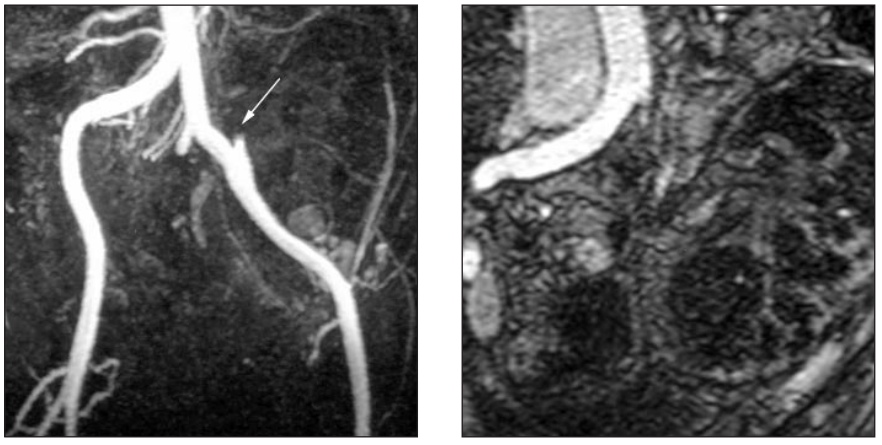

A B

Figure 13. (A) Oblique full-thickness maximum intensity projection from a renal artery MRA performed in a renal transplant patient with abdominal pain and rising creatinine 2 weeks following a motor vehicle accident. The arrow shows the occluded transplant renal artery. **(B)** A delayed phase source image shows near complete absence of renal blood flow. The graft could not be salvaged.

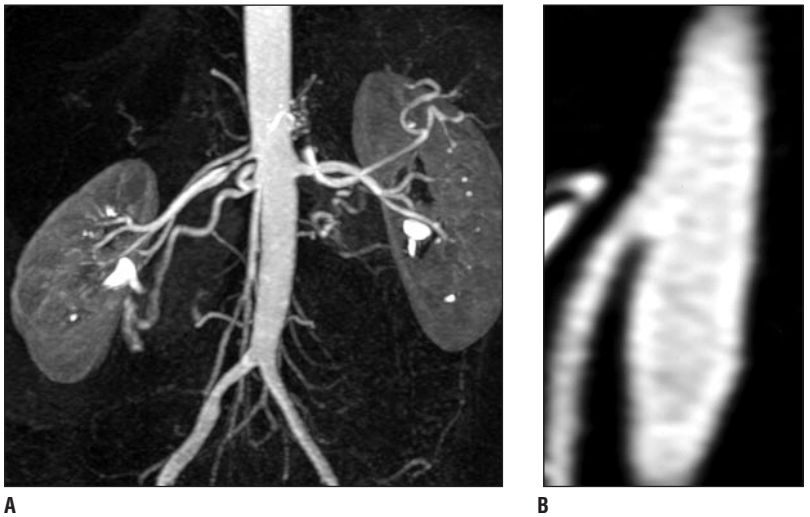

A B

Figure 14. (A) Full-thickness coronal maximum intensity projection (MIP) from an abdominal MRA. **(B)** The sagittal subvolume MIP demonstrates incidental complete occlusion of the proximal celiac axis. Note the long moderate main right renal artery stenosis with poststenotic dilatation.

teric ischemia or tumor encasement, are performed in either the coronal or sagittal plane, and are better suited to evaluating the more proximal vessels.[113,114] Slice thickness should be similar to that of a renal artery study (less than approximately 2.4 mm), particularly when using the coronal plane, as the proximal mesenteric arteries travel primarily anteriorly. Keep in mind that the hepatic, gastroduodenal, and distal superior mesenteric arteries may be further anterior than is usually included in a renal study, and, therefore, volume coverage will need to be increased (or shifted anteriorly) in order to see these structures.

Portal/Hepatic Veins

Portal venous or hepatic vein studies are performed in a coronal plane with a phased-array body coil (Figure 15).[115] Slice thickness can be increased to approximately 3 mm to adequately cover the relevant portal venous structures. Axial bright-blood scout images, such as true FISP, are useful for determining the anterior and posterior extent of the portal/hepatic veins, and may even be diagnostic.

With portal venous and hepatic venous studies, timing is not as crucial as with arterial studies, since the portal venous phase is longer and thus easier to isolate. After obtaining the arterial phase images, which allow for arterial evaluation, an approximately 10-sec pause allows the patient to recover from the breath-hold. Imaging is then repeated, followed by a second pause and a third scan. In this manner, the second set of images usually provides a nice portal venous and hepatic venous phase. The third set may show collaterals to better advantage.

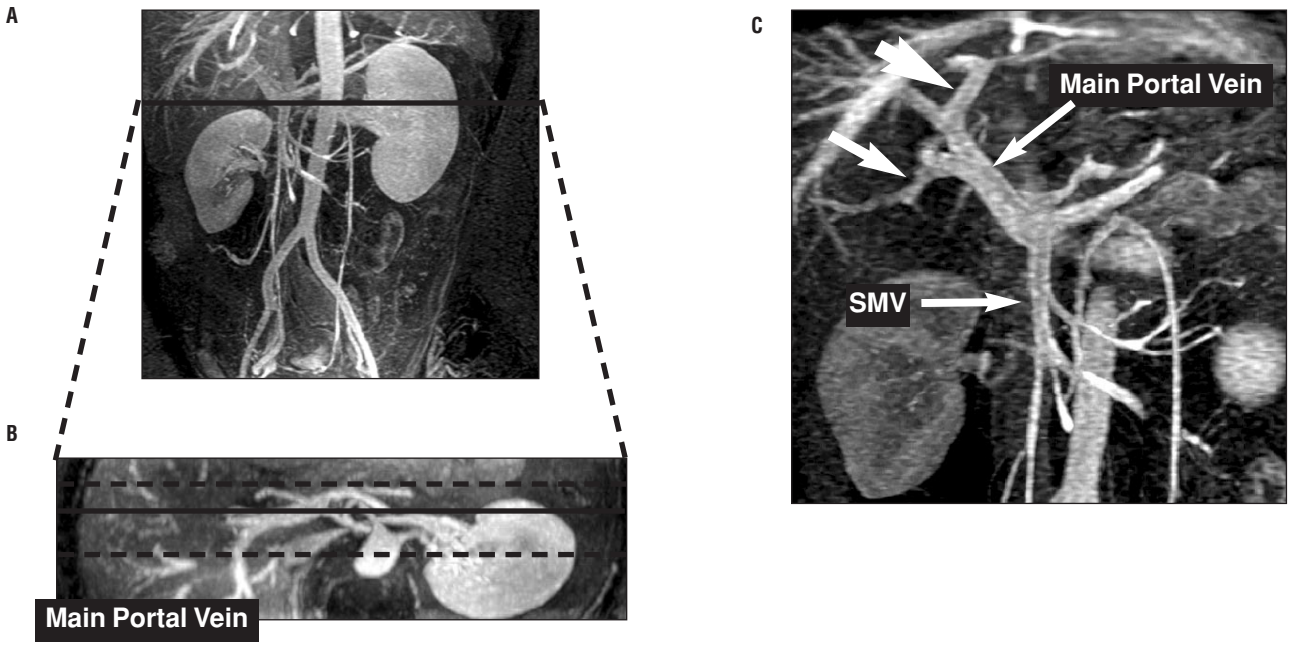

Figure 15. Coronal 3D Gd MRA of portal vein with 20 mL Gd-BOPTA. **(A)** Coronal MIP of entire volume. **(B)** Axial reformation through portal vein with dotted lines indicating optimal volume for performing subvolume MIP. **(C)** Subvolume MIP shows portal vein to better advantage by excluding more posterior structures. Note anomalous posterior division of right portal vein (small arrow) arising prior to left portal vein (large arrow).

This protocol has the added advantage of essentially being a dynamic liver study. Hence if there is concern over a hepatic mass, this can be evaluated dynamically, provided it is included in the imaging volume.[116] Under these circumstances, further delayed phases should be obtained out to 5 or 10 minutes.

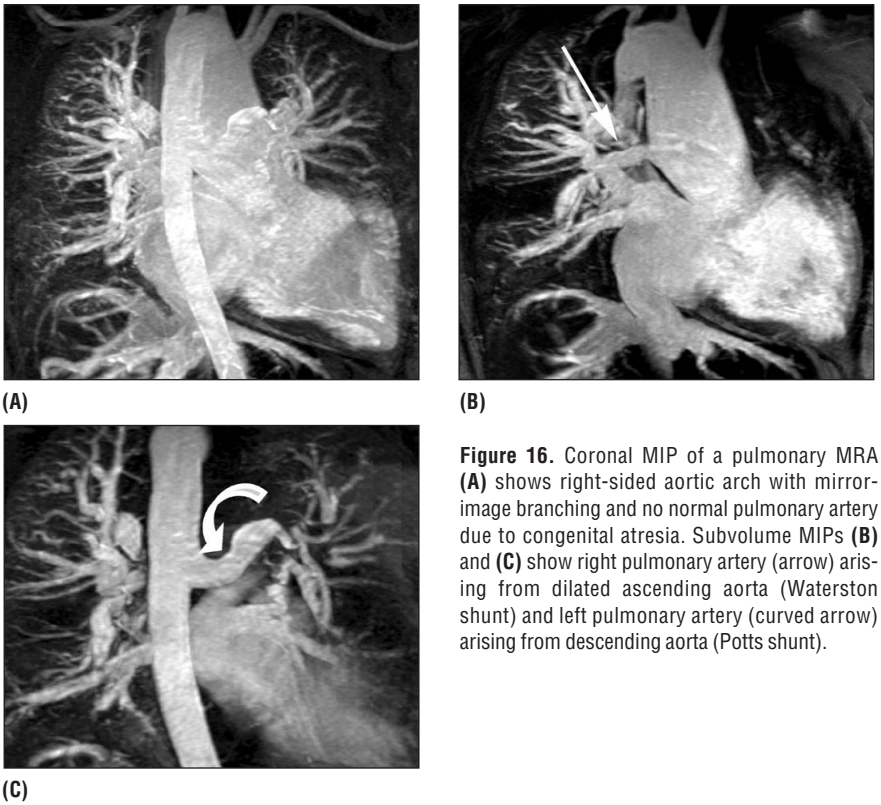

Figure 16. Coronal MIP of a pulmonary MRA **(A)** shows right-sided aortic arch with mirror-image branching and no normal pulmonary artery due to congenital atresia. Subvolume MIPs **(B)** and **(C)** show right pulmonary artery (arrow) arising from dilated ascending aorta (Waterston shunt) and left pulmonary artery (curved arrow) arising from descending aorta (Potts shunt).

Pulmonary Arteries

Three-dimensional CE- MRA of the pulmonary arteries is gaining acceptance (Figure 16). A recent large-scale study comparing MRA with conventional digital subtraction angiogrphy (DSA) suggests that pulmonary MRA is similar in accuracy to that of helical CT, being sensitive and specific for emboli in segmental and larger vessels.[117] Creating high-quality pulmonary MR angiograms, however, requires considerable care. Good breath-holding or extremely short acquisition times are extremely important, and, unfortunately, many patients who require pulmonary angiography are significantly respiratory compromised and therefore cannot breath-hold well. A phased-array body coil should be used whenever possible.

The exam must be tailored to the individual patient. Two approaches can be used—single-acquisition coronal, and double-acquisition sagittal (sepa-

A

B

C

D

Figure 17. Carotid MRA. **(A)** The full-thickness maximum intensity projection (MIP) demonstrates the great vessels extending from the arch, although there is some signal drop-off due to the coil. **(B)** Right and **(C)** left sagittal subvolume MIPs demonstrate occlusion and high-grade stenosis of the internal carotid arteries, respectively. **(D)** Note also the high-grade left vertebral artery "tandem" stenosis in the coronal subvolume MIP.

rate injections and acquisitions for each lung).[117,118] Which approach to use is a matter of preference, breath-hold capability, and machine speed. For the double-acquisition sagittal approach, the volume coverage for each acquisition is smaller, and a high degree of rectangular FOV can be used. This reduces acquisition time, or alternatively, allows for increased spatial resolution (as compared with a single coronal acquisition). In addition, the arms can remain by the patient's side, as the fold-over direction is anterior-posterior. On the down side, two separate acquisitions require more scanner and postprocessing time and more contrast, and the pulmonary trunk and proximal pulmonary arteries may be excluded (although this is not usually clinically relevant).

For either approach, a total slab thickness of 100 to 150 mm is typical, with true slice thickness optimally <2.6 mm.[118] Frequency FOV is typically 300 to 360 mm, depending on patient size, with a higher degree of rectangular FOV possible for the sagittal approach (approximately 45% to 70% versus approximately 65% to 70%). Matrix size should be on the order of 320×160, such that overall resolution is $<1.0 \times 2.0 \times 2.6$ mm. We always perform at least one practice run to evaluate the patient's breath-holding capability, ensure the patient will comply with the breathing instructions, and check that any fold-over is acceptable.

For a TR of 5 msec, acquisition times for coronal and sagittal acquisitions will be approximately 25 and 20 sec, respectively. Shorter scan times are certainly desirable, especially given the difficulty these patients often have with breath-holding and the cardiac motion within the chest. We expect increased use of high temporal resolution techniques in the immediate future.[73,82] Correct bolus timing is important, but not as essential as it is for other vascular territories. It is difficult to isolate the pulmonary arterial phase from the pulmonary venous phase, although this is possible with extremely high temporal resolution or correlation analysis.[77] Fortunately, however, this is not a big problem, as pulmonary arteries and veins are easily distinguished on coronal images. The main pulmonary artery should be used for fluoroscopic triggering or calibrating a timing bolus. If these techniques are unavailable, transit time is typically 5 to 15 sec. Gadolinium doses are approximately double dose for coronal imaging and single dose per side for sagittal imaging.

Extracranial Carotid Arteries

Carotid CE-MRA is typically performed using a single contrast injec-

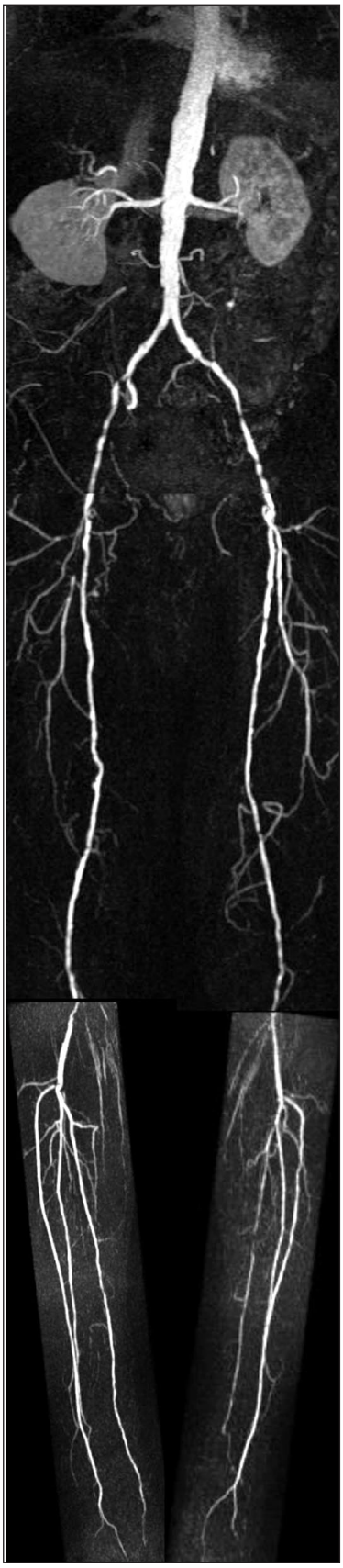

A

B

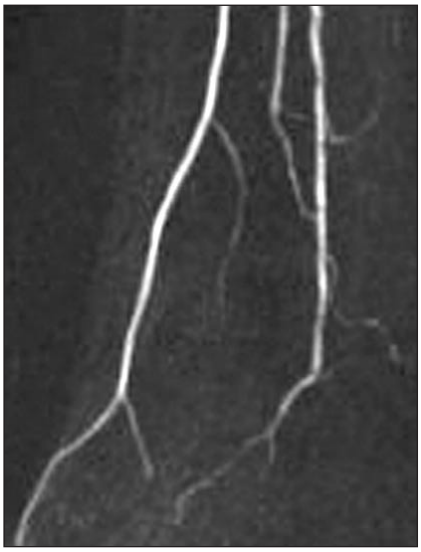

C

D

Figure 18. (A) Composite coronal maximum intensity projection (MIP) from a three-station peripheral moving-table MRA performed for bilateral calf claudication. The upper and middle stations were performed in a coronal plane, each requiring <12 sec. The lower station was acquired as 2 sagittal slabs with true 1-mm isotropic resolution and required 70 sec. This allowed for inclusion of the pedal arteries. The upper and lower stations were performed using SENSE. Note the extensive disease throughout the arterial structures, with bilateral high-grade stenoses of the external iliac arteries. **(B)** The 1-mm isotropic lower station resolution provides excellent anatomic detail of the trifurcation (coronal subvolume MIP) and **(C)** right and **(D)** left pedal arteries. These subvolume MIPs show the dorsalis pedis arteries are widely patent bilaterally, but the left posterior tibial artery is occluded distally, with the right lateral plantar artery occluded at its origin.

tion in the coronal plane (Figure 17). More so than in any other vascular territory, elliptical centric phase-encoding order and nearly perfect timing is required to isolate the arterial phase, as jugular venous enhancement can severely degrade arterial evaluation.[63] This is due to the unique characteristics of the intracranial circulation, with its short arteriovenous window (4 to 6 sec), and the blood brain barrier, which prevents significant extraction of contrast (Figure 5C). While one would expect shorter acquisition times (high temporal resolution) to increase the likelihood of isolating a pure arterial phase, excellent results have been achieved with long imaging times (40 sec to > 2 min) and high spatial resolution in combination with elliptical centric phase encoding.[63,79,83,119]

To accurately characterize a carotid stenosis according to North American Symptomatic Carotid Endarterectomy Trial (NASCET) criteria, particularly one with tortuous anatomy and high-speed turbulent jets, an accurate measurement of stenotic diameter is required.[120] Given this, we suggest true 1-mm isotropic or better resolution, using as short a TE as practical to decrease signal dephasing in the often very turbulent stenotic lumen. To maintain adequate SNR at these high resolutions, a birdcage or phased-array

coil is necessary. Unfortunately, depending on patient habitus, older neck coils suffer severe sensitivity drop-off near the arch, making evaluation of the important great vessel origins a problem (Figure 17A). Recent coil advances (combination birdcage and anterior-posterior surface coils), however, make reliable evaluation of this important region possible as part of a routine carotid examination.[83]

An FOV of 360 × 180 mm typically works well, allowing visualization down to the arch. The problem of arm aliasing into the chest is minimized due to inherent coil drop-off laterally, although this must be considered when using the built-in body coil (which is not suggested). A total slab thickness of 50 to 65 mm is usually adequate. Two-dimensional TOF or true FISP images can be used to evaluate the extent of the vertebral and carotid arteries for localization to ensure the CE-MRA volume is minimized. Typical scan parameters might be 384 × 384 × 60 matrix with 1-mm slice thickness (reconstructed to 512 × 512 × 120), for a true resolution of 0.9 × 0.9 × 1.0 mm. For a TR of 5 msec, acquisition time for such a sequence would be approximately 50 sec. Carotid artery MRA is an exception to our general rule that injection time should be on the order of 50% to 60% of acquisition time, as rapid recirculation of contrast seems to support the longer acquisition times for the high-resolution sequences. We suggest 20 to 30 mL of Gd at 1.5 to 3.0 mL/sec. As stated previously, breath-holding may help for evaluation of the arch vessels but is not necessary for the carotid arteries.[88]

Peripheral MRA

The restricted FOV inherent to MR scanners has limited CE-MRA to analyzing only 400- to 500-mm chunks of vascular anatomy at one time. While this is acceptable for carotid, aortic, renal, pulmonary, and mesenteric studies, it has made peripheral CE-MRA studies challenging. While multiple injections and multiple acquisitions with intervening table movement can be performed,[121] a recent revolutionary advance has eliminated the FOV barrier. By moving the table while scanning, a single bolus of contrast can be imaged multiple times as it flows down the legs (Figure 18).[122-124] This "moving-table" or "bolus-chase" approach allows arterial imaging from the abdominal aorta to the mid-foot in just a few minutes, and is available in different variations commercially. Even whole-body MRA using a single injection has been described.[125]

Once the FOV issue for peripheral MRA has been addressed, two further obstacles must be overcome. First, spatial resolution must be adequate for operative planning, as below-the-knee arteries are on the order of 2 to 3 mm, and grafting to an inadequate vessel can be a clinical disaster. In general, the upper- (abdominal) and middle- (thigh) station vessels are relatively large, and resolution requirements are not as strict as in the lower- (calves/feet) station, where vessels may be only 2 to 3 mm. Thus, spatial resolutions on the order of those previously discussed for the aorta and visceral arteries, with true 2.5 to 3.0 mm through plane resolution, are likely adequate in the upper and middle stations. The lower station, however, requires spatial resolution more in keeping with a carotid examination, with true 1-mm isotropic resolution an attainable goal.[92] The craniocaudal FOV for each station must be approximately 420 to 480 mm with at least 30 mm of overlap between stations.

The second obstacle is that of venous enhancement, which must be absent or minimal, as the numerous paired veins in the leg can easily obscure and confuse the arterial anatomy. It seems surprising that numerous early works demonstrated the complete lack of venous enhancement in the majority of cases, even though acquisition in the lower station did not begin until approximately 60 sec after initiating upper-station acquisition.[123,124,126] Several investigators have begun to explore this issue, which seems to be a complicated function of imaging delay, contrast injection rate, and patient-specific parameters (particularly the presence/absence of claudication versus inflammatory conditions).[127,128] Of these, it is likely patient pathology that plays the largest role. In general, patients with claudication do not demonstrate significant venous enhancement until quite late. Patients with rest pain or inflammatory conditions, such as ulcers, cellulitis, or osteomyelitis, tend to have early venous enhancement, likely secondary to arteriovenous shunting and increased perfusion. The trick then is to tailor the examination to the patient. We have begun using a 2-mL timing bolus in the calf to look for the presence of venous enhancement, and if present, to determine the length of the arteriovenous window.

We suggest the following protocol. If the patient has claudication or a timing study that indicates late venous enhancement, perform a moving-table study with coronal upper and middle stations, and either a coronal or sagittal (two slabs—one for each calf/foot—allows for easier coverage and easily includes the pedal vessels[129]) lower station study. Every attempt should be made to image the upper and middle stations quickly (short TR, SENSE, rapid table movement, etc.) so that acquisition of the lower station begins as soon as possible, decreasing chances of venous enhancement.[47] Lower station acquisition can, and should, be relatively lengthy, with spatial resolution at or near 1 mm isotropic and scan times > 1 minute very acceptable.[47,130] Phase-encoding orders should be reverse linear, linear, and elliptical centric, respectively. This ensures adequate filling of the distal upper and middle stations (external iliac and proximal femoral arteries, popliteal arteries), and suppresses lower-station venous enhancement. We typically use 40 mL of Gd with a biphasic bolus and flouroscopic triggering at the upper station (although a timing bolus will work equally well). Depending on acquisition time and table movement delay, an initial gadolinium infusion rate of 1.2 to

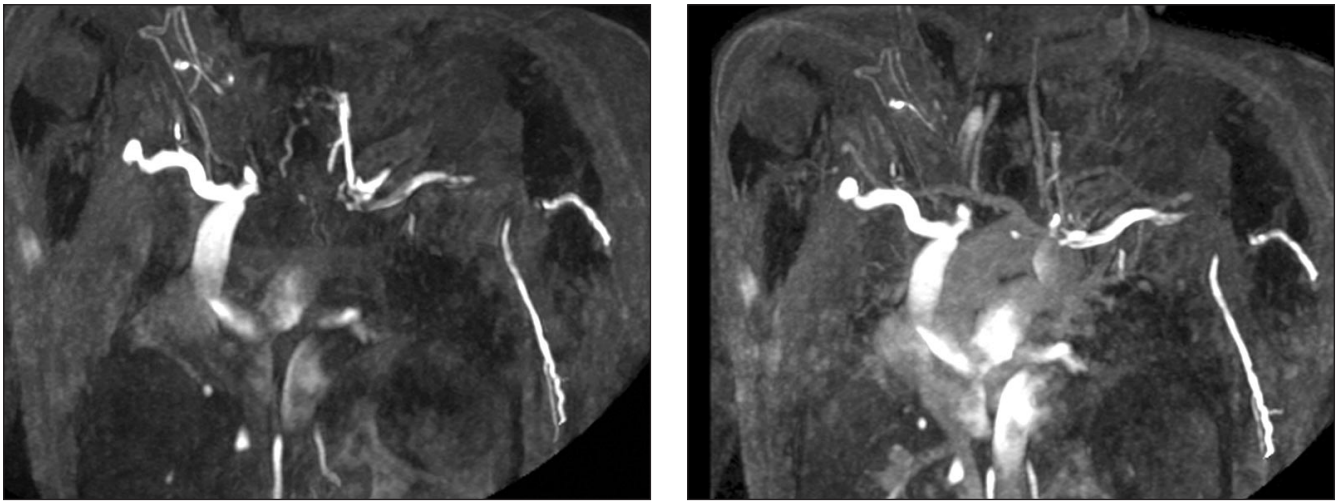

A B

Figure 19. (A) Early and **(B)** delayed subvolume maximum intensity projections from a CE-MRV study where dilute (1:12.5) gadolinium was infused bilaterally into the antecubital veins. Note the complete occlusion of the left innominate vein, with high-grade stenosis at the confluence of the right innominate vein and SVC. The left subclavian vein signal void is secondary to slab positioning.

1.8 mL/sec (20 mL) followed by 0.8 to 1.2 mL/sec (remaining 20 mL) works well. When determining bolus injection rates, consider that arterial flow down the diseased leg averages approximately 6 cm/sec, such that travel time from aorta to foot is of the order of 15 to 20 sec.[47,131] Also consider that the bolus broadens significantly, and like the carotid, recirculation of contrast appears to be quite adequate for supporting high-resolution, long acquisitions in the lower station.

If, on the other hand, the patient has distal rest pain or inflammatory disease, or demonstrates rapid venous enhancement on a lower extremity test bolus, we suggest two separate injections. The first injection should target only the lower station, with parameters similar to those of a moving-table examination, timing from the test bolus (flouroscopic triggering difficult in the lower leg), and use of 15 mL of Gd at a rate of 0.8 to

Table 1. MRI Vascular Contrast Agent Classification*

	Paramagnetic		*Superparamagnetic*	
No protein interaction	*Weak protein interaction*	*Strong protein interaction*	*Macromolecular*	*USPIO*
Gadopentetate dimeglumine (Gd-DTPA; Magnevist®)	Gadobenate dimeglumine (Gd-BOPTA; MultiHance®)	MS-325	P792 AMI 227	SH U 555A (Resovist®)
Gadoteridol (Gd-HP-DO3A; ProHance®)		B-22956	Gadomer-17	NC100150
Gadodiamide (Gd-DTPA-BMA; Omniscan®)				
Gadoversetamide (Gd-DTPA-BMEA; Optimark®)				
Gadoterate meglumine (Gd-DOTA; Dotarem®)				
Gadobutrol (Gd-BT-DO3A; Gadovist®)				

*Classification scheme for "vascular" magnetic resonance imaging (MRI) contrast agents. The paramagnetic gadolinium chelates can be classified according to their degree of protein interaction. The ultra-small iron oxide particles (USPIO) are "blood pool agents" that demonstrate long intravascular enhancement. Table based on data from Knopp M, von Tengg-Kobligk H, Floemer F, Schoenberg S. Contrast agents for MRA: Future directions. *J Magn Reson Imaging.* 1999;10:314-316.[136]
Manufacturer information: MS-325, EPIX Medical, Cambridge, MA; Resovist, Schering AG, Berlin, Germany; Magnevist, Schering AG/Berlex Imaging, Wayne, NJ; Multihance, Bracco Imaging, Milano, Italy/Bracco Diagnostics, Princeton, NJ; Prohance, Bracco Imaging /Bracco Diagnostics; NC100150, Amersham Health, Oslo, Norway; Omniscan, Amersham Health, Oslo, Norway; Optimark, Mallinckrodt, St. Louis, MO; Dotarem, Guerbet, Aulnay-Sous-Bois, France; Schering AG, Berlin, Germany.

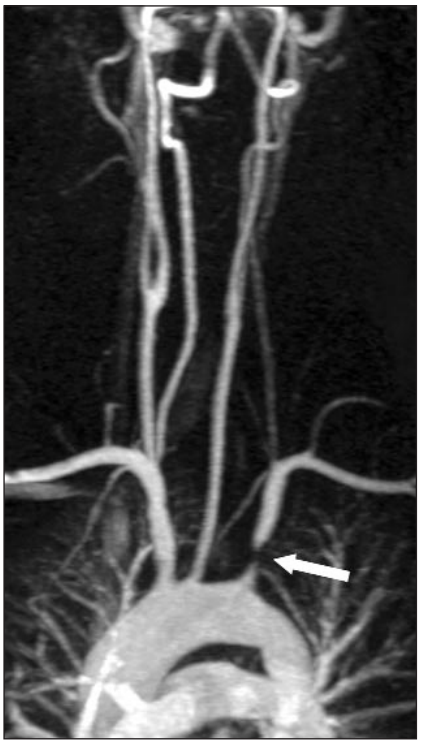

Figure 20. The full-thickness maximum intensity projection (0.1 mmol/kg Gd-BOPTA) shows occlusion of the left subclavian artery (arrow) with collateralization from the left vertebral artery. The patient presented with typical clinical symptoms, and interventional therapy was performed. Due to the clear depiction of the size of the narrowed lumen, an interventional procedure could be accurately planned. (Images courtesy of Günther Schneider, Department of Diagnostic Radiology, University Hospital, Homburg/Saar, Germany.)

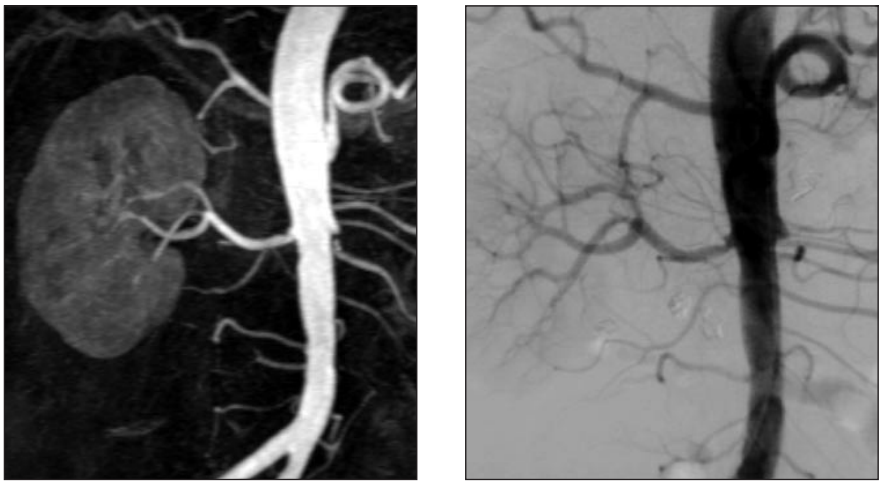

A **B**

Figure 21. A 64-year-old patient after left-side nephrectomy with newly developed arterial hypertension. **(A)** The full-thickness maximum intensity projection reveals a proximal renal artery stenosis with slight poststenotic dilatation of the vessel. **(B)** The corresponding DSA examination performed during interventional therapy confirms the stenosis. Note the excellent depiction of smaller vessels on the MRA image and the good correlation with DSA. (Images courtesy of Günther Schneider, Department of Diagnostic Radiology, University Hospital, Homburg/Saar, Germany.)

1.0 mL/sec. A second injection of 25 mL (1.2 to 1.8 mL/sec) can then be performed to evaluate the upper and middle stations as a two-station moving-table examination. Regardless of the technique used, subtraction is extremely important, particularly in the lower extremities, and a precontrast mask should always be obtained.[40] For the two-injection technique, subtraction becomes an absolute necessity following the second injection.

MR VENOGRAMS

Gadolinium-enhanced MR venograms can be performed in a manner similar to a conventional contrast venogram.[132,133] By injecting a dilute Gd solution directly into the peripheral veins (arm or leg) during 3D image acquisition, structures such as the subclavian veins, superior vena cava (SVC), and IVC can be evaluated (Figure 19). This provides much greater venous enhancement than the venous phase of an arterial study, since the Gd is delivered to the veins in a much higher concentration (less dilution of the bolus and no extravasation into extravascular structures). The arterial enhancement is also less than on the venous phase of a typical contrast MRA study, although such delayed phases can be effective as well.[134]

We find that diluting one bottle (20 mL) of Gd into a 250 mL bag of saline (1:12.5) works well when injected into a peripheral vein at 2 to 3 mL/sec. Multiple veins can be injected simultaneously, as in Figure 19. Imaging delay is not terribly important, as the dilute Gd solution can be delivered in large volumes. Volume coverage and slice thickness must be tailored to the individual case, and multiple phases should be obtained.

FUTURE DIRECTIONS—CONTRAST AGENTS

First-Pass Gadolinium Agents

Currently, the most widely used contrast agents in the United States, Europe, and elsewhere for first-pass CE-MRA are the "conventional" gadolinium chelates (Table 1). These are available as 0.5 Molar formulations and possess T1 relaxivities (1.5 T) between 4.3 and 5.0 $sec^{-1} \cdot mmol^{-1}$.[135] The similar concentrations and relaxation properties of these agents generally translate into similar vascular imaging performance when injected at equal doses.

Recently, a number of gadolinium chelates have been developed that possess properties advantageous for first-pass CE-MRA.[136] These include conventional Gd agents formulated at 1.0 Molar rather than 0.5 Molar (ie, gadobutrol), and agents with higher in vivo relaxivity due to a capacity for weak protein interaction (ie, gadobenate dimeglumine [Gd-BOPTA]). In the case of gadobutrol, studies have shown that the higher concentration of Gd

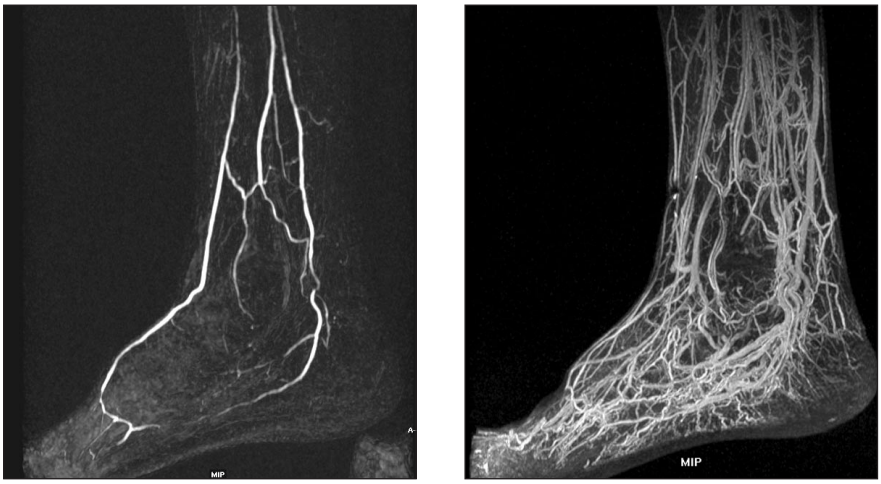

A B

Figure 22. Contrast-enhanced MRA (CE-MRA) of the foot using the blood-pool agent MS-325 in a patient with ischemic rest pain. **(A)** Arterial and **(B)** equilibrium sagittal full-volume maximum intensity projections, MS-325 dose 0.05 mmol/kg. The arterial study is subtracted, 46 sec in duration, with true voxel size of $0.9 \times 0.9 \times 1.8$ mm^3. The equilibrium study is fat suppressed at a delay of 5 minutes, 4:57 in duration, with a true voxel size $0.9 \times 0.9 \times 0.8$ mm^3.

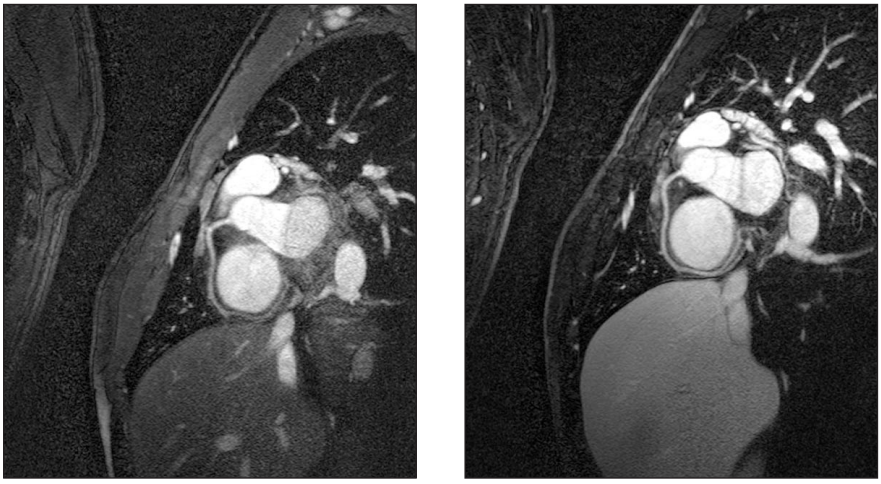

A B

Figure 23. B22956 in imaging of healthy right coronary artery. **(A)** Unenhanced (T2Prep acquisition) and **(B)** B22956-enhanced (0.075 mmol/kg) image acquired at 25-min postcontrast using 3D Navigator gated and corrected inversion recovery-fast field echo (IR-FFE) sequence. (Images courtesy of Eckart Fleck and Ingo Paetsch, German Heart Institute, Berlin, Germany; Matthias Stuber, Beth Israel Deaconess Medical Center, Cardiovascular Division, Boston, MA; and Friedrich Cavagna, Bracco Imaging SpA, Milan, Italy.)

combined with a more rapid bolus enables greater intravascular signal than is achievable with equivalent doses of traditional agents.[137-139] This may prove useful for the improved visualization of smaller arteries in vascular regions in which the SNR is limited, such as in the calf and distal renal arteries. Improved visualization of smaller pelvic vessels has already been reported.[139]

Gadobenate dimeglumine also demonstrates increased intravascular signal as compared with conventional gadolinium chelates (Table 1).[139-141] This agent differs from the other available Gd agents in that it possesses a higher in vivo T1 relaxivity (9.7 $sec^{-1} \cdot mmol^{-1}$) due to weak and transient interactions between the Gd-BOPTA chelate and serum proteins, particularly albumin.[135,142] Clinical benefits of the increased relaxivity have been demonstrated for all vascular territories, including the peripheral vasculature.[143-145] Specifically, there is better visualization of lesions in larger vessels (Figure 20), as well as better depiction of smaller vessels themselves (Figure 21). Like the conventional nonprotein-interacting gadolinium chelates, gadobenate dimeglumine demonstrates an excellent safety profile.[146]

"Blood Pool" Gadolinium Agents

Because of the rapid redistribution of the first-pass gadolinium chelates into the extracellular compartment, various attempts have been made to formulate intravascular blood-pool contrast agents for 3D CE-MRA. Currently, two main types of intravascular agents based on Gd are under development: Agents that differ from the purely extracellular and weakly protein-interacting agents in having strong affinity for serum albumin (Table 1), and macromolecular agents whose size precludes their rapid extravasation (Table 1). Although no agents are yet approved for clinical use, two examples of agents with strong affinity for serum proteins are currently undergoing clinical trials: MS-325[147-149] (Figure 22) and B22956[150,151] (Figure 23). Both of these agents appear very promising, with excellent safety profiles and the capacity to perform conventional high-quality first-pass dynamic imaging in addition to delayed steady-state vascular imaging. This may be particularly useful for coronary studies.[150,152,153]

Examples of Gd-based blood pool agents with macromolecular structures are gadomer-17[154] and P792.[155] Like MS-325 and B22956, preliminary results suggest these agents may prove beneficial for coronary MRA.[156,157]

Figure 24. NC100150 (5.0 mg Fe/kg bodyweight, slow hand injection, third injection of an accumulating dose scheme) reveals occlusion of the left renal artery and a 60% to 70% stenosis of the right renal artery.

Superparamagnetic Iron Oxide Agents

The second major category of potential contrast agents for MRA consists of the superparamagnetic group, which is based on ultra-small particles of iron oxide (USPIO) (Table 1). Currently, SH U 555A is the only clinically approved USPIO agent available for CE-MRA, although few studies have been conducted in vascular territories other than the upper abdomen.[158] AMI 227 is another potentially useful representative of this group, although, again, few studies have been conducted.[159]

Perhaps the most promising of the USPIO agents currently under development is the blood-pool agent NC100150 (Figure 24).[160,161] As with the Gd blood-pool agents, the potential advantages of this agent include a long intravascular half-life with minimal leakage into the interstitial space, thereby permitting the steady-state vascular imaging. Preliminary studies on the use of this agent for coronary MRA have already been reported,[161] and work is ongoing to establish its potential for other applications such as renal perfusion.[162]

As it stands today, the imaging quality achievable with first-pass agents has, to some extent, eliminated the initial target role for intravascular agents. It has become apparent that real benefits will most likely only be clinically achievable if the intravascular agents can be used both for first-pass and steady-state imaging. Nevertheless, it is doubtful that this type of blood-pool agent will ever have any advantage over the currently available Gd agents for dynamic, arterial-phase MRA. Conceivably, this type of agent may have benefits for ultra-high–resolution imaging, for assessment of vasculature during intervention, and for real-time therapy monitoring. Other opportunities that may present themselves include perfusion applications combined with first-pass imaging.

While MR angiography using blood-pool agents may ultimately prove beneficial, all current clinical work utilizes extracellular gadolinium chelates.

FUTURE DIRECTIONS—HARDWARE

Among the most important recent developments in MR hardware has been the introduction of whole body 3.0-T scanners. The principal advantage of increasing the magnetic field strength is improved SNR, resulting in better resolution and conspicuity of vessels using similar acquisition times.[163] Although clinical experience with CE-MRA at 3.0 T is somewhat limited at present, early studies have indicated markedly improved performance of unenhanced TOF techniques, particularly in imaging of the intracranial and cervical vasculature.[163,164] Similarly, imaging at 3.0 T has been reported to improve the resolution and delineation of small venous vessels in the brain,[165] and appears advantageous for contrast-enhanced vascular and coronary imaging.[166-168] It remains to be seen just how the availability of 3.0 T machines will impact CE-MRA. Several challenges remain to be overcome, including developing new coils, overcoming specific absorption rate (radiofrequency power deposition) limitations, and optimizing protocols. This aside, however, it appears likely the SNR-derived improvement in spatial and temporal resolution at 3.0 T will lead to significant improvements in CE-MRA image quality.

CONCLUSION

Contrast-enhanced MRA provides a safe, fast, and cost-efficient alternative to conventional diagnostic angiography throughout the vasculature. Numerous recent advances allow for high-resolution breath-hold and multistation imaging with optimal arterial phase contrast bolus timing. As the technique is further refined, better coils, better contrast agents, and perhaps higher magnetic field strengths will allow for greater spatial and temporal resolution, further increasing the effectiveness and utility of CE-MRA.

REFERENCES

1. Saloner D. MRA: Principles and display. In: Higgins C, Hricak H, Helms C, eds. *Magnetic Resonance Imaging of the Body*. Philadelphia: Lippencott-Raven; 1997:1345-1368.
2. Gullberg G, Wherli F, Shimakawa A, Simmons M. MR vascular imaging with a fast gradient refocusing pulse sequence and reformatted images from transaxial sections. *Radiology.* 1997;165: 241-246.
3. Doumolin C, Cline H, Souza S, et al. Three-dimensional time-of-flight magnetic resonance angiography using spin saturation. *Magn Reson Imaging.* 1989;11:35-46.
4. Owen R, Baum R, Carpenter J, et al. Symptomatic peripheral vascular disease: Selection of imaging parameters and clinical evaluation with MR angiography. *Radiology.* 1993;187:627-635.
5. Cortell E, Kaufman J, Geller S, et al. MR angiography of the tibial runoff vessels: Imaging with the head coil compared to conventional arteriography. *AJR Am J Roentgenol.* 1996;167:147-151.

6. Glickerman D, Obregon G, Schmiedl U, et al. Cardiac-gated MR angiography of the entire lower extremity: A prospective comparison with conventional angiography. *AJR Am J Roentgenol.* 1996;167:445-451.
7. Patel P, Kuntz K, Klufas R, et al. Carotid bifurcation. Can magnetic resonance angiography and duplex ultrasonography replace contrast arteriography? *Stroke.* 1995;26:1753-1758.
8. Anderson C. MRA of the aortic arch and extracranial carotid arteries. In: Higgins C, Hricak H, Helms C, eds. *Magnetic Resonance Imaging of the Body.* Philadelphia, Pa: Lippencott-Raven; 1997:1369-1381.
9. Blatter D, Parker D, Robinson R. Cerebral MR angiography with multiple overlapping thin slab acquisition. *Radiology.* 1991;179:805-811.
10. Kim D, Edelman R, Kent K, et al. Abdominal aorta and renal artery stenosis: Evaluation with MR angiography. *Radiology.* 1990;174:727-731.
11. Yucel E, Kaufman J, Prince M, et al. Time-of-flight renal MR arteriography: Utility in patients with renal insufficeincy. *Magn Reson Imaging.* 1993;11:925-930.
12. Loubeyre P, Cahan R, Grozel F, et. al. Transplant renal artery stenosis. Evaluation of diagnosis with magnetic resonance angiography compared with color duplex sonography and arteriography. *Transplantation* 1996; 62:446-450.
13. Prince M. Body MR angiography with gadolinium contrast agents. *MRI Clin N Am.* 1996; 4:11-24.
14. Prince M. Gadolinium-enhanced MR aortography. *Radiology.* 1994; 191:155-164.
15. Bryant D, Payne J, Firmin D, Longmore D. Measurement of flow with NMR imaging using a gradient pulse and phase difference technique. *Comput Assist Tomogr.* 1984;8:588-593.
16. Gedroyc W. Magnetic resonance angiography of renal arteries. *Urol Clin North Am.* 1994; 21:201-214.
17. Bass J, Prince M, Londy F, Chenevert T. Effect of gadolinium on phase-contrast MR angiography of the renal arteries. *AJR Am J Roentgenol.* 1997; 168:261-266.
18. Gedroyc W, Negus R, Al-Kutoubi A, et al. Magnetic resonance angiography of renal transplants. *Lancet.* 1992;339:789-791.
19. Yucel E. Magnetic resonance angiography of the lower extremity and renal arteries. *Sem Ultrasound CT MRI.* 1992;13:291-302.
20. Ngheim H, Winter R, Mountford M, et al. Evaluation of the portal venous system before liver transplantation: value of phase-contrast MR angiography. *AJR Am J Roentgenol.* 1995;164: 871-878.
21. Lundin B, Cooper T, Meyer R, Potchen E. Measurement of total and unilateral renal blood flow by oblique-angle velocity encoded 2D-CINE magnetic resonance angiography. *Magn Reson Med.* 1992;11:51-59.
22. Schoenberg S, Knopp M, Londy F, et al. Renal artery stenosis: Stenosis grading by combined morphologic and functional MR imaging: Results of a multicenter multireader analysis. *J Am Soc Nephrol.* 2002;13:158-169.
23. Weinman H, Brasch R, Press W, Wesbey G. Charcteristics of gadolinium-DTAP complex: A potential NMR contrast agent. *AJR Am J Roentgenol.* 1984;142:619-624.
24. Schima W, Mukerjee A, Saini S. Contrast-enhanced MR imaging. *Clin Radiol.* 1996;51:235-244.
25. Goldstein H, Kashanian F, Blumetti R, et al. Safety assessment of gadopentetate dimeglumine in U.S. clinical trials. *Radiology.* 1990;174:17-23.
26. Niendorf H, Haustein J, Alhassan A, Clauss W. Safety of gadolinium-DTPA: Extended clinical experience. Presented as part of Brasch R, mod. Workshop on Contrast-Enhanced Magnetic Resonance. Society for Magnetic Resonance in Medicine Meeting, Napa, CA, 1991:70-79.
27. Haustein J, Niendorf H, Krestin G, et al. Renal tolerance of gadolinium-DTAP/dimeglumine in patients with chronic renal failure. *Invest Radiol.* 1992; 27:153-156.
28. Prince M, Arnoldus C, Frisoli J. Nephrotoxicity of high dose gadolinium compared to iodinated contrast. *J Magn Reson Imaging.* 1996;6:162-166.
29. Hohenschuh E, Watson A. Theory and mechanisms of contrast-enhancing agents. In: Higgins C, Hricak H, Helms C, eds. *Magnetic Resonance Imaging of the Body.* Philadelphia, Pa: Lippencott-Raven; 1997:1439-1464.
30. Prince M, Yucel E, Kaufman J, et al. Dynamic gadolinium-enhanced three-dimensional abdominal MR arterography. *JMRI.* 1993;3:877-881.
31. Runge V, Kirsch J, Lee C. Contrast-enhance MR angiography. *JMRI.* 1993;3:233-239.
32. Ehman R, Revel D, Sievers R, Brasch R. Acute myocardial ischemia. Magnetic resonance contrast enhancement with gadolinium-DTPA. *Radiology.* 1984;153:157-163.
33. Moseley M, Sawyer A. Imgaing Techniques: Pulse sequences. In: Higgins C, Hricak H, Helms C, eds. *Magnetic Resonance Imaging of the Body.* Philadelphia, Pa: Lippencott-Raven; 1997:43-69.
34. Wehrli F. Principles of magnetic resonance. In: Stark D, Bradley W, eds. *Magnetic Resonance Imaging.* St. Louis, MO: Mosby-Year Book; 1992:3-20.
35. Prince M, Narasimham D, Stanley J, et al. Breath-hold gadolinium-enhanced MR angiography of the abdominal aorta and its major branches. *Radiology.* 1995;197:785-792.
36. Snidow J, Johnson S, Harris V, et al. Three-dimensional gadolinium-enhanced MR angiography for aortoiliac inflow assessment plus renal artery screening in a single breath hold. *Radiology.* 1996;198:725-732.
37. Leung D, McKinnon G, Davis C, et al. Breath-hold, contrast-enhanced, three-dimensional MR angiography. *Radiology.* 1996;201:569-571.
38. Hendrick R, Roff U. *Image contrast and noise.* Chicago, Il: Mosby Yearbook; 1991.
39. Weinman H, Laniado M, Mutzel W. Pharmacokinetics of Gd-DTPA/dimeglumine after intravenous injection into healthy volunteers. *Physiol Chem Phys Med NMR.* 1984;16:167-172.
40. Lee V, Flyer M, Weinreb J, et al. Image subtraction in gadolinium-enhanced MR imaging. *AJR Am J Roentgenol.* 1996;167:1427-1432.
41. Maki J, Chenevert T, Prince M. Optimizing three-dimensional gadolinium-enhanced MR angiography. *Invest Radiol.* 1998;33:528-537.
42. Verhoeven L. Digital subtraction angiography: The technique and an analysis of the physical factors influencing the image quality [thesis]. In: Delft: *Technische Hogeschule*; 1985.
43. Barnes G, Lakshminarayann A. Conventional and spiral Computed Tomography. In: Lee J, Sagel S, Stanley R, Heiken J, eds. *Computed Body Tomgraphy with MRI Corellation.* Philadelphia, Pa: Lippencott-Raven; 1998:1-20.
44. Maki J, Prince M, Londy F, Chenevert T. The effects of time varying intravascular signal intensity on three-dimensional MR angiography image quality. *J Magn Reson Imaging.* 1996;6:642-651.
45. Riederer S, Tasciyan T, Farzaneh F. MR flouroscopy: Technical feasibility. *Magn Reson Med.* 1988;8:1-15.
46. Fain S, Riederer S, Bernstein M, Huston J. Theoretical limits of spatial resolution in elliptical-centric contrast-enhanced 3d-MRA. *Magn Reson Med.* 1999;42:1106-1116.
47. Maki J, Wilson G, Eubank W, Hoogeveen R. Utilizing SENSE to achieve lower station sub-millimeter isotropic resolution and minimal venous enhancement in peripheral MR angiography. *J Magn Reson Imaging.* 2002;15:484-491.
48. Bampton A, Riederer S, Korin H. Centric phase-encoding order in three-dimensional MP-RAGE sequences: Application to abdominal imaging. *J Magn Reson Imaging.* 1992;2:327-334.
49. Wilman A, Riederer S. Improved centric phase encoding orders for three-dimensional magnetization-prepared MR angiography. *Magn Reson Med.* 1996;36:384-392.
50. Maki J, Chenevert T, Prince M. The effects of incomplete breath holding on 3D MR image quality. *J Magn Reson Imaging.* 1997;7:1132-1139.
51. Wilman A, Riederer S, Breen J, Ehman R. Elliptical spiral phase-encoding order: An optimal, field-of-view-dependent ordering scheme for breath-hold contrast-enhanced 3D MR angiography. *Radiology.* 1996;201:328-329.
52. Hany T, Schmidt M, Hilfiker P, et al. Optimization of contrast dosage for gadolinium-enhanced 3D MRA of the pulmonary and renal arteries. *Magn Reson Imaging.* 1998;16:901-906.
53. Shetty A, Bis K, Kirsch M, et al. Contrast-enhanced breath-hold three-dimensional magnetic resonance angiography in the evaluation of renal arteries: Optimization of technique and pitfalls. *J Magn Reson Imaging.* 2000;12:912-923.
54. Snidow J, Aisen A, Harris V, et al. Iliac artery MR angiography: Comparison of three-dimensional gadolinium-enhanced and two-dimensional time-of-flight techniques. *Radiology.* 1995;196: 371-378.
55. Steiner P, Debatin J, Romanowski B, et al. Optimization of breath-hold 3D MR pulmonary angiography [abstract]. *Radiology.* 1996;201(P): 201.

56. Hany T, Debatin J, Schmidt M, et al. Three-dimensional MR angiography of the renal arteries in a single breath-hold. *Radiology.* 1996; 201:218.
57. Finn J, Baskaran V, Carr J, et al. Thorax: Low-dose contrast-enhanced three-dimensional MR angiography with subsecond temporal resolution initial results. *Radiology.* 2002;224:896-904.
58. Prince M, Grist T, Debatin *J. 3D contrast MR angiography.* Berlin: Springer-Verlag; 1997.
59. Earls J, Rofsky N, DeCorato D, et al. Breath-hold single-dose gadolinium-enhanced three-dimensional MR aortography: Usefulness of a timing examination and MR power injector. *Radiology.* 1996:705-710.
60. Krinsky G, Rofsky N, Flyer M, et al. Gadolinium-enhanced three-dimensional MR angiography of acquired arch vessel disease. *AJR Am J Roentgenol.* 1996;167:981-987.
61. Kreitner K, Kunz R, Kalden P, et al. Contrast-enhanced three-dimensional MR angiography of the thoracic aorta: Experiences after 118 examinations with a standard dose contrast administration and different injection protocols. *Eur Radiol.* 2001;11:1355-1363.
62. Wilman A, Riederer S, King B, et al. Flouroscopically-triggered contrast-enhanced three dimensional MR angiography with elliptical centric view order: Application to the renal arteries. *Radiology.* 1997;205:137-146.
63. Huston J, Fain S, Riederer S, Wilman A, Bernstein M, Busse R. Carotid arteries: Maximizing arterial to venous contrast in fluoroscopically triggered contrast-enhanced MR angiography with elliptic centric view ordering. *Radiology.* 1999;211:265-273.
64. Fellner F, Fellner C, Wutke R, et al. Fluoroscopically triggered contrast-enhanced 3D MR DSA and 3D time-of-flight turbo MRA of the carotid arteries: First clinical experiences in correlation with ultrasound, x-ray angiography, and endarterectomy findings. *Magn Reson Imaging.* 2000;18:575-585.
65. Watts R, Wang Y, Redd B, et al. Recessed elliptical-centric view-ordering for contrast-enhanced 3D MR angiography of the carotid arteries. *Magn Reson Med.* 2002;48:419-424.
66. Levy R, Maki J. Three-dimensional contrast-enhanced MR angiography of the extracranial carotid arteries: Two techniques. *AJNR Am J Neuroradiol.* 1998;19:688-690.
67. Korosec F, Grist T, Frayne R, Mistretta C. Time-resolved contrast-enhanced 3D MR angiography. *Magn Reson Med.* 1996;36:345-351.
68. Mistretta C, Grist T, Korosec F, Frayne R. 3D time-resolved contrast-enhanced MR DSA: Advantages and tradeoffs. *Magn Reson Med.* 1998;40:571-581.
69. Schoenberg S, Bock M, Floemer F, et al. High-resolution pulmonary arterio- and venography using multiple-bolus multiphase 3D-Gd-MRA. *J Magn Reson Imaging.* 1999;10:339-346.
70. Schoenberg S, Essig M, Hallscheidt P, et al. Multiphase magnetic resonance angiography of the abdominal and pelvic arteries: Results of a bicenter multireader analysis. *Invest Radiol.* 2002;37:20-28.
71. Stein B, DeMarco J, Zhou Y. 3D Time-resolved MRA with elliptic centric view ordering. Initial clinical experience to evaluate tibo-peroneal arteries. Presented at the XIIIth Annual Inernational Workshop on MRA. Madison, WI, 2001.
72. Hennig J, Scheffler K, Laubenberger J, Strecker R. Time-resolved projection angiography after bolus injection of contrast agent. *Magn Reson Med.* 1997;37:341-345.
73. Goyen M, Laub G, Ladd M, et al. Dynamic 3D MR angiography of the pulmonary arteries in under four seconds. *J Magn Reson Imaging.* 2001;13:372-377.
74. Finn J, Carr J, Pereles S, et al. Time-resolved, contrast-enhanced MR angiography of the thorax. Presented at the XIIIth Annual International Workshop on MRA. Madison, WI, 2001.
75. Pruessmann K, Weiger M, Scheidegger M, Boesiger P. SENSE: Sensitivity encoding for fast MRI. *Magn Reson Med.* 1999;42:952-962.
76. Finn J, Larson A, Moore J, Simonetti O. Subsecond 3D contrast-enhanced MRA of the thorax with radial k-space sampling. Presented at the Xth Scientific Meeting and Exhibition of the International Society for Magnetic Resonance in Medicine. Honolulu, HI, 2002.
77. Bock M, Schoenberg S, Floemer F, Schad L. Separation of arteries and veins in 3D MR angiography using correlation analysis. *Magn Reson Med.* 2000;43:481-487.
78. Mistretta C, Grist T, Frayne R, Korosec F. Contrast and motion artifacts in 4D MR angiography. *Radiology.* 1996;201:238.
79. Turski P, Korosec F, Carroll T, et al. Contrast-Enhanced magnetic resonance angiography of the carotid bifurcation using the time-resolved imaging of contrast kinetics (TRICKS) technique. *Top Magn Reson Imaging.* 2001;12:175-181.
80. Mazaheri Y, Carroll T, Du J, et al. Combined time-resolved and high-spatial-resolution 3D MRA using an extended adaptive acquisition. *J Magn Reson Imaging.* 2002;15:291-301.
81. Peters D, Korosec F, Grist T, et al. Undersampled projection reconstruction applied to MR angiography. *Magn Reson Med.* 2000;43:91-101.
82. Barger A, Block W, Toropov Y, et al. Time-resolved contrast-enhanced imaging with isotropic resolution and broad coverage using an undersampled 3D projection trajectory. *Magn Reson Med.* 2002;48:297-305.
83. Willinek W, Gieseke J, Von Falkenhousen V, et al. CD-3D MRA of the supraaoritc arteries at 512 and 1024 matrix: The use of randomly segmented central k-space ordering (CENTRA). Presented at the Xth Scientific Meeting and Exhibiton of the International Society for Magnetic Resonance in Medicine. Honolulu, HI, 2002.
84. Wood M, Runge V, Henkelman R. Overcoming motion in abdominal MR imaging. *AJR Am J Roentgenol.* 1988;150:513-522.
85. Ehman R, Felmlee J. Adaptive technique for high-definition MR imaging of moving structure. *Radiology.* 1989;173:255-263.
86. Vasbinder G, Maki J, Nijenhuis R, et al. Motion of the distal renal artery during 3D contrast-enhanced breath-hold MRA. *J Magnetic Reson Imaging.* 2002;16:685-696.
87. Holland G, Dougherty L, Carpenter J, et al. Breath-hold ultrafast three-dimensional gadolinium-enhanced MR angiography of the aorta and the renal and other visceral abdominal arteries. *AJR Am J Roentgenol.* 1996;166:971-981.
88. Carr J, Ma J, Desphande V, et al. High-resolution breath-hold contrast-enhanced MR angiography of the entire carotid circulation. *AJR Am J Roentgenol.* 2002;178:543-549.
89. Weiger M, Pruessmann K, Kassner A, et al. Contrast-enhanced 3D MRA using SENSE. *J Magn Reson Imaging.* 2000;12:671-677.
90. Sodickson D, Manning W. Simultaneous acquisition of spatial harmonics (SMASH): Fast imaging with radiofrequency coil arrays. *Magn Reson Med.* 1997;38:591-603.
91. Wilson G, Maki J, Evitts M, et al. A direct comparison study to evaluate the usefulness of Sensitivity Encoding (SENSE) in evaluating renal artery stenosis using MR angiography. Presented at the XIII Annual International Workshop on MRA. Madison, WI. 2001.
92. Maki J, Wilson G, Hoogeveen R. 3D Gd enhanced moving table MR angiography of the aorta and outflow vessels using SENSE to achieve high resolution of the below knee vasculature. Presented at the Seventh scientific meeting of the International Society for Magnetic Resonance in Medicine, Glasgow, Scotland, 2001.
93. Du Y, Parker D, Davis W, Gao T. Reduction of partial-volume artifacts with zero-filled interpolation in three-dimensional MR angiography. *J Magn Reson.* 1994;4:733-741.
94. Ros P, Gauger J, Stoupis C, et al. Diagnosis of renal artery stenosis: Feasibility of combining MR angiography, MR renography, and gadopentetate-based measurements of glomerular filtration rate. *AJR Am J Roentgenol.* 1995;165:1447-1451.
95. Schoenberg S, Bock M, Aumann S, et al. Quantitative recording of renal function with magnetic resonance tomography. *Radiologe.* 2000; 40:925-937.
96. De Marco J, Nesbit G, Wesbey G, Richardson D. Prospective evaluation of extracranial carotid stenosis: MR angiography with maximum-intensity projections and multiplanar reformation compared with conventional angiography. *AJR Am J Roentgenol.* 1994;163:1205-1212.
97. Laub G. Displays for MR angiography. *Magn Reson Med.* 1990;14:222-229.
98. Rossnick S, Laub G, Braeckle R. Three dimensional display of blood vessels in MRI. In: *Proceedings of the IEEE: Computers in Cardiology*. New York: IEEE; 1986:193-195.
99. Anderson C, Saloner D, Tsuruda J, et al. Artifacts in maximum intensity projection display of MR angiograms. *AJR Am J Roentgenol.* 1990; 154:623-629.
100. Baskaran V, Pereles F, Nemcek AJ, et al. Gadolinium-enhanced 3D MR angiography of renal artery stenosis: A pilot comparison of maxi-

mum intensity projection, multiplanar reformatting, and 3D volume-rendering postprocessing algorithms. *Acad Radiol.* 2002;9:50-59.
101. Douek P, Revel D, Chazel S, et al. Fast MR angiography of the aortoiliac arteries and arteries of the lower extremity: Value of bolus-enhanced, whole-volume subraction technique. *AJR Am J Roentgenol.* 1995;165:431-437.
102. Wang Y, Johnston DL, Breen JF, et al. Dynamic MR digital subtraction angiography using contrast enhancement, fast data acquisition, and complex subtraction. *Magn Reson Med.* 1996;36:551-556.
103. Wang Y, Winchester P, Khilnani N, et al. Contrast-enhanced peripheral MR angiography from the abdominal aorta to the pedal arteries: Combined dynamic two-dimensional and bolus-chase three-dimensional acquisitions. *Invest Radiol.* 2001;36:170-177.
104. Hoogeveen R, Bakker C, Viergever M. Limits to the accuracy of vessel diameter measurement in MR angiography. J Magn Reson Imaging. 1998;8:1228-1235.
105. Wilson G, Haynor D, Maki J. Resolution requirements for grading stenoses in 3D CE-MRA. Presented at the Sixth scientific meeting of the International Society for Magnetic Resonance in Medicine. Denver, CO, 2000.
106. Stafford-Johnson D, Hamilton B, Dong Q, et al. Vascular Complications of Liver Transplantation: Evlauation with gadolinium-enhanced MR angiography. *Radiology.* 1998;207:153-160.
107. Wutke R, Lang W, Fellner C, et al. High-resolution, contrast-enhanced magnetic resonance angiography with elliptical centric k-space ordering of supra-aortic arteries compared with selective X-ray angiography. *Stroke.* 2002;33:1522-1529.
108. Murray J, Manisali M, Flamm S, et al. Intramural hematoma of the thoracic aorta: MR image findings and their prognostic implications. *Radiology.* 1997;204:349-355.
109. Prince M, Schoenberg S, Ward J, et al. Hemodynamically significant atherosclerotic renal artery stenosis: MR angiographic features. *Radiology.* 1997;205:128-136.
110. Hood M, Ho V, Corse W. Three-dimensional phase-contrast magnetic resonance angiography: A useful clinical adjunct to gadolinium-enhanced three-dimensional renal magnetic resonance angiography? *Mil Med.* 2002; 167:343-349.
111. Johnson D, Lerner C, Prince M, et al. Gadolinium-enhanced magnetic resonance angiography of renal transplants. *Magn Reson Imaging.* 1997;15:13-20.
112. Ferreiros J, Mendez R, Jorquera M, et al. Using gadolinium-enhanced three-dimensional MR angiography to assess arterial inflow stenosis after kidney transplantation. *AJR Am J Roentgenol.* 1999;172:751-757.
113. Laissy J, Trillaud H, Douek P. MR angiography: noninvasive vascular imaging of the abdomen. *Abdom Imaging.* 2002;27:488-506.
114. Baden J, Racy D, Grist T. Contrast-enhanced three-dimensional magnetic resonance angiography of the mesenteric vasculature. *J Magn Reson Imaging.* 1999;10:369-375.
115. Stafford-Johnson D, Chenevert T, Cho K, Prince M. Portal venous magnetic resonance angiography. A review. *Acad Radiol.* 1998;5:289-305.
116. Rofsky N, Lee V, Laub G, et al. Abdominal MR imaging with a volumetric interpolated breath-hold examination. *Radiology.* 1999;212:876-884.
117. Oudkerk M, van Beek E, Wielopolski P, et al. Comparison of contrast-enhanced magnetic resonance angiography and conventional pulmonary angiography for the diagnosis of pulmonary embolism: a prospective study. *Lancet.* 2002; 359:1643-1647.
118. Meaney J, Johansson L, Ahlstrom H, Prince M. Pulmonary magnetic resonance angiography. *J Magn Reson Imaging.* 1999;10:326-338.
119. Wikstrom J, Johansson L, Rossitti S, et al. High resolution carotid artery MRA. Comparison with fast dynamic acquistion and duplex ultrasound scanning. *Acta Radiol.* 2002;43:256-261.
120. North American Symptomatic Carotid Endarterectomy Trial Collaborators. Beneficial effect of carotid endarterectomy in symptomatic patients with high-grade carotid stenosis. *N Engl J Med.* 1991;325:445-453.
121. Sueyoshi E, Sakamoto I, Matsuoka Y, et al. Aortoiliac and lower extremity arteries: Comparison of three-dimensional dynamic contrast-enhanced subtraction MR angiography and conventional angiography. *Radiology.* 1999;210:683-688.
122. Ho K, Leiner T, DeHaan M, et al. Peripheral vascular tree stenoses: evaluation with moving-bed infusion-tracking MR angiography. *Radiology.* 1998;206:683-692.
123. Meaney J, Ridgway J, Chakraverty S, et al. Stepping-table gadolinium-enhanced digital subtraction MR angiography of the aorta and lower extremity arteries: Preliminary experience. *Radiology.* 1999;211:59-67.
124. Ho V, Choyke P, Foo T, et al. Automated bolus chase peripheral MR angiography: Initial practical experiences and future directions of this work-in-progress. *J Magn Reson Imaging.* 1999;10:376-388.
125. Goyen M, Quick H, Debatin J, et al. Whole-body three-dimensional MR angiography with a rolling table platform: Initial clinical experience. *Radiology.* 2002;224:270-277.
126. Ho K, de Haan M, Kessels A, et al. Peripheral vascular tree stenoses: Detection with subtracted and nonsubtracted MR angiography. *Radiology.* 1998;206:673-681.
127. Ho K. *Thesis: MR Angiography of the Lower Extremities.* Maastricht, The Netherlands: University of Maastricht; 1999:93-108.
128. Ho K. First experiences with BPA for peripheral MRA. Presented at the XI International Workshop on MRA. Lund, Sweden, 1999.
129. Maki J, Wilson G, Eubank W, et al. 3D Gd-enhanced moving table peripheral MR angiography using multi-station SENSE to include the pedal vasculature. Presented at the Tenth Scientific Meeting and Exhibition of the International Society for Magnetic Resonance in Medicine. Honolulu, HI, 2002.
130. Leiner T, Kessels A, van Engelshoven J. Total runoff peripheral MRA in patients with critical ischemia and tissue loss can detect more patent arteries than IA-DSA. In: *Tenth Scientific Meeting and Exhibition: International Society for Magnetic Resonance in Medicine.* 2002;210.
131. Wang Y, Lee H, Avakian R, et al. Timing alogrithm for bolus chase MR digital subtraction angiography. *Magn Reson Med.* 1998;39:691-696.
132. Ruehm S, Zimny K, Debatin J. Direct contrast-enhanced 3D MR venography. *Eur Radiol.* 2001;11:102-112.
133. Li W, Kaplan D, Edelman R. Three-diensional low dose gadolinium-enhanced peripheral MR venography. *J Magn Reson Imaging.* 1998;8:630-633.
134. Thornton M, Ryan R, Varghese J, et al. A three-dimensional gadolinium-enhanced MR venography technique for imaging central veins. *AJR Am J Roentgenol.* 1999;173:999-1003.
135. de Haën C, Cabrini M, Akhnana L, et al. Gadobenate dimeglumine 0.5 M solution for injection (MultiHance) pharmaceutical formulation and physicochemical properties of a new magnetic resonance imaging contrast medium. *J Comput Assist Tomogr.* 1999;23 Suppl 1:S161-S168.
136. Knopp M, von Tengg-Kobligk H, Floemer F, Schoenberg S. Contrast agents for MRA: Future directions. *J Magn Reson Imaging.* 1999;10:314-316.
137. Tombach B, Reimer P, Prumer B, et al. Does a higher concentration of gadolinium chelates improve first-pass cardiac signal changes? *J Magn Reson Imaging.* 1999;10:806-812.
138. Goyen M, Lauenstein T, Herborn C, et al. 0.5 M Gd chelate (Magnevist) versus 1.0 M Gd chelate (Gadovist): Dose-independent effect on image quality of pelvic three-dimensional MR-angiography. *J Magn Reson Imaging.* 2001;14:602-607.
139. Herborn C, Lauenstein T, Ruehm S, et al. Intraindividual comparison of gadopentetate dimeglumine, gadobenate dimeglumine and gadobutro for pelvic 3D magnetic resonance angiography. *Invest Radiol.* 2003;38:27-33.
140. Knopp M, Schoenberg S, Rehm C, et al. Assessment of gadobenate dimeglumine (Gd-BOPTA) for MR angiography: Phase I studies. *Invest Radiol.* 2002;37:706-715.
141. Völk M, Strotzer M, Lenhart M, et al. Renal time-resolved MR angiography: Quantitative comparison of gadobenate dimeglumine and gadopentetate dimeglumine with different doses. *Radiology.* 2001;220:484-488.
142. Cavagna F, Maggioni F, Castelli P, et al. Gadolinium chelates with weak binding to serum proteins. A new class of high-efficiency, general purpose contrast agents for magnetic resonance imaging. *Invest Radiol.* 1997;32:780-796.
143. Kroencke T, Wasser M, Pattynama P, et al. Gadobenate dimeglumine-enhanced magnetic res-

onance angiography of the abdominal aorta and renal arteries. *AJR Am J Roentgenol.* 2002;179: 1573-1582.
144. Ruehm S, Goyen M, Barkhausen J, et al. Rapid magnetic resonance angiography for detection of atherosclerosis. *Lancet.* 2001;357:1086-1091.
145. Goyen M, Herborn C, Lauenstein T, et al. Optimization of contrast dosage for gadobenate dimeglumine-enhanced high-resolution whole body 3D MR angiography. *Invest Radiol.* 2002; 37:263-268.
146. Kirchin M, Pirovano G, Venetianer C, Spinazzi A. Safety assessment of gadobenate dimeglumine (Multihance): Extended clinical experience from phase I studies to post-marketing surveillance. *J Magn Reson Imaging.* 2001;14: 281-294.
147. Grist T, Korosec F, Peters D, et al. Steady-state and dynamic MR angiography with MS-325: Initial experience in humans. *Radiology.* 1998; 207:539-544.
148. Lauffer R, Parmelee D, Dunham S, et al. MS-325: Albumin-targeted contrast agent for MR angiography. *Radiology.* 1998;207:529-538.
149. Bluemke D, Stillman A, Bis K, et al. Carotid MR angiography: Phase II study of safety and efficacy of MS-325. *Radiology.* 2001;219: 114-122.
150. La Noce A, Stoelben S, Scheffler K, et al. B22956/1, a new intravascular contrast agent for MRI: First administration to humans-preliminary results. *Acad Radiol.* 2002;9 Suppl:S404-406.
151. Zheng J, Li D, Cavagna F, et al. Contrast-enhanced coronary MR angiography: Relationship between coronary artery delineation and blood T1. *J Magn Reson Imaging.* 2001;14:348-354.
152. Stuber M, Botnar R, Danias P, et al. Contrast agent-enhanced, free-breathing, three-dimensional coronary magnetic resonance angiography. *J Magn Reson Imaging.* 1999;10:790-799.
153. Huber M, Paetsch I, Schnackenburg B, et al. Performance of a new gadolinium-based intravascular contrast agent in free-breathing inversion-recovery 3D coronary MRA. *Magn Reson Med.* 2003;49:115-121.
154. Dong Q, Hurst D, Weinmann H, et al. Magnetic resonance angiography with gadomer-17. An animal study original investigation. *Invest Radiol.* 1998;33:699-708.
155. Gaillard S, Kubiak C, Stolz C, et al. Safety and pharmacokinetics of p792, a new blood-pool agent: results of clinical testing in nonpatient volunteers. *Invest Radiol.* 2002;37:161-166.
156. Taupitz M, Schnorr J, Wagner S, et al. Coronary magnetic resonance angiography: experimental evaluation of the new rapid clearance blood pool contrast medium P792. *Magn Reson Med.* 2001;46:932-938.
157. Li D, Zheng J, Weinmann H. Contrast-enhanced MR imaging of coronary arteries: Comparison of intra- and extravascular contrast agents in swine. *Radiology.* 2001;218:670-678.
158. Reimer P, Allkemper T, Matuszewski L, Balzer T. Contrast-enhanced 3D-MRA of the upper abdomen with a bolus-injectable SPIO (SH U 555 A). *J Magn Reson Imaging.* 1999; 10:65-71.
159. Mayo-Smith W, Saini S, Slater G, et al. MR contrast material for vascular enhancement: Value of superparamagnetic iron oxide. *AJR Am J Roentgenol.* 1996;166:73-77.
160. Weishaupt D, Ruhm S, Binkert C, et al. Equilibrium-phase MR angiography of the aortoiliac and renal arteries using a blood pool contrast agent. *AJR Am J Roentgenol.* 2000;175:189-195.
161. Taylor A, Panting J, Keegan J, et al. Safety and preliminary findings with the intravascular contrast agent NC100150 injection for MR coronary angiography. *J Magn Reson Imaging.* 1999; 9:220-227.
162. Bachmann R, Conrad R, Kreft B, et al. Evaluation of a new ultrasmall superparamagnetic iron oxide contrast agent Clariscan (NC100150) for MRI of renal perfusion: Experimental study in an animal model. *J Magn Reson Imaging.* 2002; 16:190-195.
163. Campeau NG, Huston J 3rd, Bernstein MA, er al. Magnetic resonance angiography at 3.0 Tesla: Initial clinical experience. *Top Magn Reson Imaging.* 2001;12:183-204.
164. Al-Kwifi O, Emery D, Wilman A. Vessel contrast at three Tesla in time-of-flight magnetic resonance angiography of the intracranial and carotid arteries. *Magn Reson Imaging.* 2002; 20:181-187.
165. Reichenbach J, Barth M, Haacke E, et al. High-resolution MR venography at 3.0 Tesla. *J Comput Assist Tomogr.* 2000;24:949-957.
166. Hugg J, Rofsky N, Stokar S, et al. Clinical whole body MRI at 3.0 T - initial experience. Presented at the Xth Scientific Meeting and Exhibition of the ISMRM. Honolulu, HI, 2002.
167. Leiner T, Vasbinder B, De Vries M, et al. Contrast-Enhanced Peripheral MRA at 3.0T: Initial results. Presented at the 10th Scientific Meeting and Exhibition of the ISMRM. Honolulu, HI, 2002.
168. Stuber M, Botnar R, Fischer S, et al. Preliminary report on in vivo coronary MRA at 3 Tesla in humans. *Magn Reson Med.* 2002;48:425-429.

CME Information

This activity has been planned and implemented in accordance with the Essential Areas and Policies of the Accreditation Council for Continuing Medical Education (ACCME) through the joint sponsorship of the Institute for Advanced Medical Education and Anderson Publishing, Ltd. The Institute for Advanced Medical Education is accredited by the Accreditation Council for Continuing Medical Education (ACCME) to sponsor continuing medical education for physicians.

The Institute for Advanced Medical Education designates this continuing medical education activity for a maximum of 3 Category 1 credits toward the AMA Physician's Recognition Award. Each physician should claim only those credits that he/she actually spent in the activity.

See page 182 for instructions on how to participate in the program.

As of January 1, 2003, courses approved for AMA Category 1 CME credit that are relevant to the radiologic sciences are accepted for Category B CE credit on a one-to-one basis by the American Registry of Radiologic Technologists (ARRT).

In compliance with the Essentials and Standards of the ACCME, the authors of this CME tutorial are required to disclose any significant financial or other relationships they may have with the manufacturer(s) of any commercial product(s) or provider(s) of any commercial service(s) discussed in this program. Dr. Maki reports a relationship with EPIX Medical as a consultant and through research funding. Dr. Knopp reports relationships with Amersham Health, Berlex Imaging/Schering, and Bracco Diagnostics as a consultant. Dr. Prince reports relationships with TopSpins, Inc. as a major shareholder; as well as patent agreements with GE Medical Systems, Siemens Medical Systems, Mallinckrodt, Bracco Diagnostics, and Medrad, Inc.